

# Limits to positional information in boundary-driven systems

Prashant Singh<sup>1,\*</sup> and Karel Proesmans<sup>1,†</sup>

<sup>1</sup>*Niels Bohr International Academy, Niels Bohr Institute,  
University of Copenhagen, Blegdamsvej 17, 2100 Copenhagen, Denmark*

Chemical gradients can be used by a particle to determine its position. This *positional information* is of crucial importance, for example in developmental biology in the formation of patterns in an embryo. The central goal of this paper is to study the fundamental physical limits on how much positional information can be stored inside a system. To achieve this, we study positional information for boundary-driven systems, and derive, in the near-equilibrium regime, a universal expression involving only the chemical potential and density gradients of the system. We also conjecture that this expression serves as an upper bound on the positional information of boundary driven systems beyond linear response. To support this claim, we test it on a broad range of solvable boundary-driven systems.

*Introduction:* Nature endows biological matter with the astounding ability to self-organize fascinating spatio-temporal patterns that pervade across several length scales [1]. For instance, one often sees insects with their bodies divided into segments of repetitive patterns or birds and animals with unique patterns of spots and stripes. One classic mechanism of pattern formation in reaction-diffusion systems is Turing pattern [2–4]. While naively, one expects diffusion to generate uniform concentration of chemicals, Turing showed that two diffusing chemical species with distinct diffusion coefficients and activation-inhibition interplay can, under suitable condition, spontaneously break the symmetry of homogeneous concentrations and generate recurring structures such as stripes, spots, or even more complex patterns.

Another important mechanism commonly studied in the context of developing embryos is the the French-flag model [5, 6]. In order to build complex body structures, individual cells have to take decisions and adopt fates suitable for their positions. Yet cells do not have any direct way to measure their positions. The key idea in the French-flag model is that during the early developmental stage of an embryo, some specific chemicals, called ‘morphogens’ are deposited locally on one side of the embryo. These chemicals diffuse inside the embryo, thereby establishing a concentration gradient [7, 8]. Unlike in Turing patterns, the spatial symmetry is broken due to the presence of graded concentration of morphogens. Wolpert proposed that cells could determine their positions from the local morphogen concentrations within these graded profiles and take up fates correlated with their positions [5, 9]. Therefore, the graded-concentration profile of signalling morphogen provides ‘positional information’ to the cells, see Figure 1. Cells, in turn, read out these positional cues in a threshold-dependent manner and give rise to spatial patterns with distinct boundaries.

Although the idea of positional information was originally introduced in the context of developmental biology, its applications reach beyond this. For example, synthetic versions of the French-Flag model have been constructed and positional information can play a crucial

role in the construction of self-assembling soft materials, where individual components could determine their position through the chemical concentration of a signalling molecule [10–13].

Recently a mathematical framework has been developed to quantitatively study positional information [14–20]. Essentially, one defines the positional information as the amount of information one gets about the position by measuring the concentration of signal molecules in this position. Based on the information theory, this amount of information is equal to

$$\mathcal{I}_{(n,i)}(\{\rho\}) = \sum_i \int dn P(i, n) \log_2 \left[ \frac{P(i, n)}{P_i(i)P_n(n)} \right], \quad (1)$$

where  $P(i, n)$  is the joint probability distribution observing a concentration  $n$  at position  $i$  and  $P_i(i)$  and  $P_n(n)$  are the associated marginals. Throughout our paper, we have associated every lattice point with an elementary volume  $v_c$ , c.f., Fig. 1. Such a consideration may arise because, in biological experiments, the cells for which positional information is measured have a finite volume that is small compared to the overall size of the embryo.

Coming to our formula in Eq. (1), the prior distribution  $P_i(i)$  is chosen based on the the initial knowledge of the system while other probabilities are uniquely determined through the system’s dynamics. We also remark that if  $n$  takes only discrete values, then the integration in Eq. (1) needs to be replaced appropriately by its summation. Also, we have written positional information as a function of model parameters  $\{\rho\}$  whose precise definition will be given later.

This framework has been successfully applied to biological systems. For example, experiments reveal that the four gap genes in the *Drosophila* embryo carry approximately  $\sim 4.2$  bits of information. This amount of information enables cells to know their positions within an error of  $\sim 1\%$  of the total embryo length [14]. Since position determines a cell’s fate, such precision is crucial for the robust and reproducible positioning of body structures like stripes of gene expression or cephalic

furrow, while the system functions in a noisy environment. To understand how this developmental robustness is achieved, it is important to know how much information can be carried by the morphogens, but there are, to the best of our knowledge, no results on the fundamental physical limits of how much positional information can be stored inside a system.

The central goal of this paper is to fill this gap by determining the maximal amount of positional information stored in symmetric boundary-driven discrete lattice systems, i.e., systems that are in equilibrium in the absence of boundary driving and that satisfy translational and left-right symmetry, in terms of their distance from thermodynamic equilibrium [21–27]. In particular, we will look at systems that are in contact with two particle reservoirs with chemical potentials  $\mu_L$  and  $\mu_R$  [and  $\Delta\mu = (\mu_L - \mu_R)$  being their difference]. We show that within linear response around equilibrium and under a local-equilibrium assumption, positional information takes a universal form in terms of the chemical potentials and densities at the left and right reservoirs

$$\mathcal{I}_{(n,i)}(\bar{\rho}, \Delta\rho) \approx \frac{v_c \Delta\mu \Delta\rho}{k_B T \ln 2} \text{var} \left( \frac{i}{N} \right), \quad (2)$$

where we have  $\bar{\rho} = (\rho_L + \rho_R)/2$  and  $\Delta\rho = (\rho_L - \rho_R)/2$ , with  $\rho_L$  and  $\rho_R$  the densities at the left and right reservoir respectively,  $k_B$  is the Boltzmann constant and  $T$  is the absolute temperature at which the system is kept. Furthermore, the volume  $v_c$  is an elementary volume associated with every lattice point in the system, and  $\text{var}(f_i)$  indicates the variance of a function  $f_i$  with respect to  $P_i(i)$  and  $N$  ( $\gg 1$ ) is the total number of discrete positions, c.f. Fig. 1. Although  $\bar{\rho}$  does not explicitly appear in Eq. (2), its influence is solely through  $\Delta\mu$ , which depends on both  $\bar{\rho}$  and  $\Delta\rho$ .

In the far-from-equilibrium regime, we numerically find that the equality of Eq. (2) is replaced by an inequality:

$$\mathcal{I}_{(n,i)}(\bar{\rho}, \Delta\rho) \leq \frac{v_c \Delta\mu \Delta\rho}{4 k_B T \ln 2}, \quad (3)$$

While this can be rigorously proven for any system close to equilibrium, we numerically find it to be valid even in the far-from-equilibrium condition for a broad class of systems [28]. This inequality thus provides a quantitative link between the positional information and the drive to maintain non-equilibrium and for a given driving, it tells us that there is a limit on how much positional information can be generated.

Although results (2) and (3) hold for any prior, both experiments in biological systems and synthetic biological experiments generally use a uniform distribution of cells. Experimentally, one therefore generally considers a flat prior,  $P_i(i) = 1/N$  [11, 14, 19, 20, 29]. For this case, we demonstrate numerically a tighter upper bound

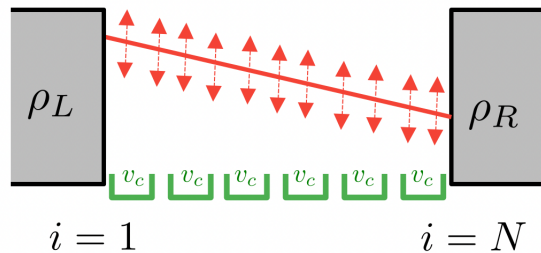


FIG. 1. Lattice sites depicted in green are in contact with two distinct reservoirs characterized by average densities  $\rho_L$  and  $\rho_R$ . Due to this coupling, the system attains a steady-state with average density profile shown by the red solid line. However, due to noise, there are fluctuations around this mean value which are indicated by dashed arrows. Positional information of a lattice site is obtained by measuring the local particle density inside a small volume  $v_c$  and employing the formula in Eq. (1).

to the positional information compared to (3)

$$\mathcal{I}_{(n,i)}(\bar{\rho}, \Delta\rho) \leq \frac{v_c \Delta\mu \Delta\rho}{12 k_B T \ln 2}. \quad (4)$$

where the equality is reached in the near-equilibrium condition, can be seen from Eq. (2) by noting  $\text{var}(i/N) \simeq 1/12$  for large  $N$ .

*Positional information near equilibrium:* We begin with a one-dimensional lattice system consisting of  $N$  sites represented by index  $i$  with  $1 \leq i \leq N$ . In bulk where  $1 < i < N$ , a particle can jump to either of its neighbouring sites with an arbitrary rate (the rate can also be a function of the number of particles in the sites). On the other hand, at the two end sites ( $i = 1$  and  $i = N$ ), the system is in contact with two particle reservoirs characterised by the average densities  $\rho_L$  and  $\rho_R$ . Without any loss of generality, we will take  $\rho_L \geq \rho_R$  throughout this paper.

Due to the coupling with the reservoirs, our lattice system eventually reaches a non-equilibrium steady-state. Our starting point is to note that even though the system as a whole is driven out-of-equilibrium, local regions can still be described, to first order in gradients, by an equilibrium measure with parameters that vary slowly across the system [30, 31]. This *local thermodynamic equilibrium* then allows us to identify thermodynamic quantities such as chemical potential locally even in out-of-equilibrium set-ups. With this idea in mind, we now consider a small volume  $v_c$  around the lattice site  $i$  and write the probability distribution to observe a number  $n$  inside this volume in the steady-state as

$$P(n|i) \sim \exp \left[ -\frac{v_c}{k_B T} (\mathcal{G}_{\mu_i}(n/v_c) - \mathcal{G}_{\mu_i}(\rho_i)) \right], \quad (5)$$

where  $\mathcal{G}_{\mu_i}(g)$  is given in terms of the Helmholtz free energy  $a(n)$  per unit volume as

$$\mathcal{G}_{\mu_i}(g) = a(g) - \mu_i g, \quad \text{and} \quad \mu_i = \left. \frac{\partial a(g)}{\partial g} \right|_{g=\rho_i}. \quad (6)$$

Here  $\mu_i$  stands for the local chemical potential which is given in terms of the local average density  $\rho_i = \langle n_i/v_c \rangle$  such that  $\rho_1 = \rho_L$  and  $\rho_N = \rho_R$ . In this description, the microscopic details of the system such as inter-particle interaction, dynamics etc, are captured by the form of free energy  $a(g)$  and the average density  $\rho_i$ . Their forms will depend on the specific model [28]. Furthermore, although we have examined discrete lattice systems in this paper, their continuum version can be derived by coarse-graining the microscopic model [24, 25]. In this context,  $v_c$  represents the coarse-graining length scale.

In general, the form of the density  $\rho_i$  can be both linear or non-linear in  $i$ . However, close to equilibrium, one generally expects it to take a linear form  $\rho_i \simeq \bar{\rho} + (1 - \frac{2i}{N}) \Delta\rho$  according to the diffusion equation. This is also in agreement with experimental observations for certain morphogens [32]. Plugging this in Eq. (5) then gives us the conditional distribution  $P(n|i)$ . Recall that we also need the joint probability distribution  $P(n, i)$  in Eq. (1). Using Bayes' theorem, we can write  $P(i, n) = P(n|i)P_i(i)$ . We now have all quantities needed in Eq. (1) and we show in [28] that the positional information is given by

$$\mathcal{I}_{(n,i)}(\bar{\rho}, \Delta\rho) \approx \frac{2\Delta\rho^2}{\ln 2 \sigma_2(\bar{\rho})} \text{var} \left( \frac{i}{N} \right), \quad (7)$$

where  $\sigma_2(\bar{\rho}) = \langle (n - \bar{\rho})^2 \rangle_{\text{eq}}$  is the variance of the density at equilibrium ( $\Delta\rho = 0$ ). As expected,  $\mathcal{I}_{(n,i)}(\bar{\rho}, \Delta\rho)$  goes to zero at equilibrium since the density remains constant across the system and therefore the chemical concentration does not correlate with position. We now establish the connection of positional information with the chemical potential difference  $\Delta\mu = (\mu_L - \mu_R)$ . Noting Eq. (6), this can be expressed in terms of the derivative of the free energy. At the leading order in  $\Delta\rho$ , we find  $\Delta\mu \sim a_2(\bar{\rho}) \Delta\rho$ , where  $a_2(\bar{\rho})$  stands for the second derivative of  $a(\bar{\rho})$ . We next use the fluctuation-response relation to write  $a_2(\bar{\rho}) = k_B T / \sigma_2(\bar{\rho}) v_c$ ; see [28] for a proof. This leads us to the expression of chemical potential difference as

$$\frac{\Delta\mu}{k_B T} \approx \frac{2\Delta\rho}{v_c \sigma_2(\bar{\rho})}. \quad (8)$$

Combining this with Eq. (7), we arrive at the universal form of the positional information quoted in Eq. (2). Moreover, we prove in [28] that the variance is bounded as  $\text{var}(i/N) \leq 1/4$  and applying this in Eq. (2), we obtain the general upper bound (3). These are the two main results of our letter. They are valid in the near-equilibrium regime for any 1-dimensional boundary-driven system

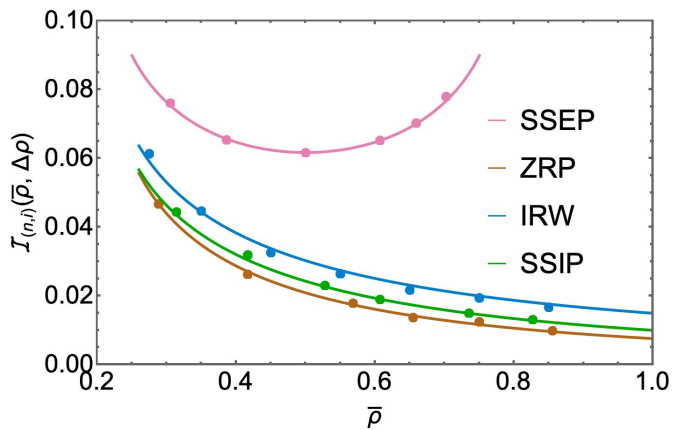


FIG. 2. Plot of the positional information as a function of  $\bar{\rho}$  for four different boundary-driven processes and its comparison with the numerical simulations. In each case, solid lines illustrate the analytical expression, c.f., summary table I in [28], while symbols denote simulation data. We have fixed the bias to  $\Delta\rho = 0.25$  and chosen a flat prior.

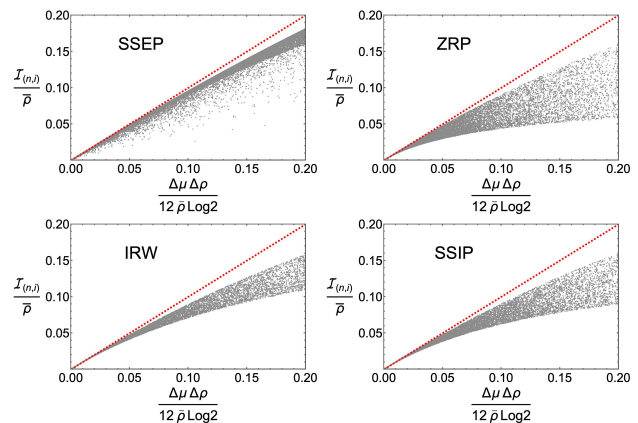


FIG. 3. Upper bound (4) on the positional information in terms of the differences  $\Delta\mu$  and  $\Delta\rho$  for four different boundary-driven processes with a flat prior. For all cases, the gray symbols are the analytical results for different random values of  $\bar{\rho}$  and  $\Delta\rho$  generated using the procedure explained in [28]. For better visibility, we have rescaled both sides of (4) by  $\bar{\rho}$  and plotted  $\mathcal{I}_{(n,i)}(\bar{\rho}, \Delta\rho) / \bar{\rho}$  vs  $\Delta\mu \Delta\rho / 12 \bar{\rho} \ln 2$ . As discussed in [28], this rescaling ensures that the near-equilibrium relation (2) is more clearly visible. The red line corresponds to the upper bound in (4). Clearly, the bound is saturated in the near-equilibrium limit. We have set  $v_c = 1$  and  $k_B T = 1$ .

with arbitrary prior probability. For the biologically relevant case,  $P_i(i) = 1/N$ , we numerically observe that the linear response result in Eq. (2) provides a further tight bound (4) to the positional information in the far-from-equilibrium regime.

*Far-from-equilibrium regime:* Up to now, our analysis has focused on the near-equilibrium situation where local thermodynamic equilibrium enabled us to derive a general bound. An immediate question that now follows is - what happens to this bound in the far-from-equilibrium

situations? Although we are unable to give an analytical proof, numerical results on a broad range of models suggest it remains valid even when the system is driven arbitrarily far from equilibrium. We will now show this for four different models, namely symmetric simple exclusion processes (SSEP), zero-range processes (ZRP), independent random walkers (IRW), and simple symmetric inclusion processes (SSIP). In the rest of our analysis, we will focus on the flat case  $P_i(i) = 1/N$  and instead test the refined bound (4) for these solvable examples. We verify (3) in the supplementary materials [28]. Furthermore, we will set  $v_c$  to the volume associated with a single lattice site and write  $k_B T = 1$  and  $v_c = 1$  in the remainder of our letter for notational simplicity.

*Example I: SSEP-* Consider the SSEP model where every lattice site can either be vacant ( $n_i = 0$ ) or be occupied by a single particle ( $n_i = 1$ ). Any particle in the bulk can jump to one of its neighbouring sites with some rate  $p$ , as long as the target site is vacant. However, dynamics at the end sites are modified due to the presence of particle reservoirs, see [28] for details. Since the occupation number  $n_i$  for this model is a binary variable, one can write the conditional probability  $P(n|i) = \rho_i \delta_{n,1} + [1 - \rho_i] \delta_{n,0}$  with density  $\rho_i = \bar{\rho} + (1 - \frac{2i}{N}) \Delta\rho$  [22–25]. If we now use this in Eq. (1), the positional information can be calculated. We have presented this expression in summary table I in [28], and validated it against numerical simulations in Figure 2. It is also consistent with our general result in Eq. (2) in the limit  $\Delta\rho \rightarrow 0$ , as one can show that  $\sigma_2(\bar{\rho}) = \bar{\rho}(1 - \bar{\rho})$ . Our objective now is to compare this expression with the chemical potential difference  $\Delta\mu$  quoted in summary table I in [28]. In Figure 3, we have plotted both  $\mathcal{I}_{(n,i)}(\bar{\rho}, \Delta\rho)$  and  $\Delta\mu\Delta\rho/12 \ln 2$  for several values of  $\bar{\rho}$  and  $\Delta\rho$ . The red dashed line represents the bound in (4). Clearly all positional information values lie below this line. In fact, for SSEP, we have rigorously proved in [28] that the bound is valid across all parameter values. Hence, our upper bound (4) holds for the SSEP arbitrarily far from the equilibrium.

*Example II: ZRP-* As a second example, we look at the boundary-driven zero-range process [26]. Unlike in SSEP, the lattice sites are now capable of accommodating an arbitrary number of particles. In bulk, a particle can jump to any of its neighbouring sites with a rate of  $pu_{n_i}$ , where  $u_{n_i}$  is a non-negative function of  $n_i$ . At the boundaries, the dynamics are modified allowing for the addition or removal of particles. For this model, the steady-state density profile is non-linear. Moreover, for the case of constant rate  $u_n = 1$ , the positional information can be calculated as shown in [28]. In Figure 2, we have compared this expression with numerical simulations and found a good agreement between them. Next we employ this result in conjunction with  $\Delta\mu$  to test the upper bound (4). As depicted in Figure 3, positional information values are situated below the red line even for this model. This ob-

servation holds true across all parameter regimes. The bound is saturated in the near-equilibrium regime where both  $\Delta\mu$  and  $\Delta\rho$  approach zero as expected. Furthermore, in this example also,  $\mathcal{I}_{(n,i)}(\bar{\rho}, \Delta\rho)$  is bounded by (4) even in the far-from equilibrium conditions.

*Example III: IRW-* Another choice of rate  $u_n = n$  corresponds to the independent, unbiased random walkers [26] and turns out to be analytically solvable. Once again, we use the positional information and chemical potential difference  $\Delta\mu$  from [28] to check our bound for this model. Plotting  $\mathcal{I}_{(n,i)}(\bar{\rho}, \Delta\rho)$  and  $(\Delta\mu\Delta\rho)/(12 \ln 2)$  in Figure 3, we have demonstrated that the upper bound is satisfied for this model. This model presents a third solvable example where the upper bound is valid in all parameter regimes.

*Example IV: SSIP-* As a final example, we investigate the simple symmetric inclusion process [33, 34]. For this model also, a lattice site can accommodate an arbitrary number of particles. However unlike the previous examples, the jump rate from  $i \rightarrow j$  [with  $j = (i \pm 1)$ ] depends on the both occupation numbers  $n_i$  and  $n_j$ . We choose the form of this rate as  $pn_i(n_j + m)$  where  $m (> 0)$  is a parameter in the model. Furthermore, the system is coupled with two reservoirs at the boundaries which drive it to a non-equilibrium steady-state. In this steady-state, we calculate the positional information and  $\Delta\mu$  as shown in [28]. These results are plotted in the bottom panel of Figure 3. From this, it is evident that the upper bound (4) is satisfied by this model. This further reinforces the conjecture that our bound holds for general boundary-driven system. Therefore, in all the examples investigated in this letter, we observe that there exists a quantitative constraint on the amount of positional information given in terms of the chemical potential and density gradients driving the system.

*Conclusions and outlook:* In conclusion, we established an important link between biophysics and non-equilibrium statistical mechanics, by studying the limits of positional information. More specifically, we derived a universal expression for the positional information  $\mathcal{I}_{(n,i)}(\bar{\rho}, \Delta\rho)$  near equilibrium, involving only the chemical potential difference and the difference in average densities driving the system. Furthermore, our analysis on several solvable models suggests that this expression serves as an upper bound on positional information in the far-from-equilibrium regime. In particular, for the case of flat prior, we find  $\mathcal{I}_{(n,i)}(\bar{\rho}, \Delta\rho) \leq v_c \Delta\rho \Delta\mu / 12 k_B T \ln 2$ . Our study indicates that there is a limit on how much positional information the morphogen particles can provide, depending on how far the system is from equilibrium, a conclusion that has profound implications for the construction of future synthetic biological systems. Given that in many experiments, the morphogen profile is measured along one dimension such as the anterior-posterior axis of the embryo [8, 14, 29] or the longitudinal axis in microchannels [10, 13], we have focused on

one-dimensional boundary-driven models and used the principle of local equilibrium to express the conditional probability in Eq. (5). However, it is possible to extend this principle even for some higher dimensional systems and our results will also be valid for them [28].

Our work paves the way for several future directions. While we examined specific models to demonstrate the bound, it remains an open problem to prove it generically. Extending this study for other models with bulk drive is an important future direction. This is especially relevant because, in some experiments, morphogen molecules experience degradation effects inside the embryo [7, 8]. Furthermore, biological systems often operate in an active non-equilibrium environment, leading to interesting phenomena such as motility-induced phase-separation [35]. Under these circumstances, the local equilibrium assumption is no longer valid, and one needs to develop new theoretical methodologies to tackle the problem [36].

We thank Jonas Berx for carefully reading the manuscript. The authors also acknowledge the support from the European Union’s Horizon 2020 research and innovation program under the Marie Skłodowska-Curie grant agreement No. 847523 ‘INTERACTIONS’ and grant agreement No. 101064626 ‘TSBC’ and from the Novo Nordisk Foundation (grant No. NNF18SA0035142 and NNF21OC0071284).

---

\* [prashantsinghramitay@gmail.com](mailto:prashantsinghramitay@gmail.com)

† [karel.proesmans@nbi.ku.dk](mailto:karel.proesmans@nbi.ku.dk)

- [1] H. Meinhardt, *Models of Biological Pattern Formation* (Academic Press, London, 1982) (1982).
- [2] A. M. Turing, The chemical basis of morphogenesis, *Philosophical Transactions of the Royal Society of London. Series B, Biological Sciences* **237**, 37 (1952).
- [3] G. Falasco, R. Rao, and M. Esposito, Information thermodynamics of turing patterns, *Physical Review Letters* **121**, 108301 (2018).
- [4] S. Rana and A. C. Barato, Precision and dissipation of a stochastic turing pattern, *Physical Review E* **102**, 032135 (2020).
- [5] L. Wolpert, Positional information and the spatial pattern of cellular differentiation, *Journal of Theoretical Biology* **25**, 1 (1969).
- [6] J. Sharpe, Wolpert’s French Flag: what’s the problem?, *Development* **146**, dev185967 (2019).
- [7] T. Gregor, W. Bialek, R. R. de Ruyter van Steveninck, D. W. Tank, and E. F. Wieschaus, Diffusion and scaling during early embryonic pattern formation, *Proceedings of the National Academy of Sciences* **102**, 18403 (2005).
- [8] V. Grieneisen, B. Scheres, P. Hogeweg, and A. Maree, Morphogengeneering roots: Comparing mechanisms of morphogen gradient formation, *BMC Systems Biology* **6**, 37 (2012).
- [9] L. Wolpert, Positional information and pattern formation, *Current Topics in Developmental Biology* **117**, 597 (2016), (Essays on Developmental Biology, Edited by P. M. Wassarman).
- [10] A. Zadorin, Y. Rondelez, G. Gines, V. Dilhas, A. Zambrano, J.-C. Galas, and A. Estevez-Torres, Synthesis and materialization of a reaction-diffusion french flag pattern, *Nature Chemistry* **9**, 990 (2017).
- [11] A. Baccouche, K. Montagne, A. Padirac, T. Fujii, and Y. Rondelez, Dynamic dna-toolbox reaction circuits: A walkthrough, *Methods* **67**, 234 (2014).
- [12] S. Toda, W. L. McKeithan, T. J. Hakkinen, P. Lopez, O. D. Klein, and W. A. Lim, Engineering synthetic morphogen systems that can program multicellular patterning, *Science* **370**, 327 (2020).
- [13] A. Dupin, L. Aufinger, I. Styazhkin, F. Rothfischer, B. K. Kaufmann, S. Schwarz, N. Galensowske, H. Clausen-Schaumann, and F. C. Simmel, Synthetic cell-based materials extract positional information from morphogen gradients, *Science Advances* **8**, eabl9228 (2022).
- [14] J. O. Dubuis, G. Tkačik, E. F. Wieschaus, T. Gregor, and W. Bialek, Positional information, in bits, *Proceedings of the National Academy of Sciences* **110**, 16301 (2013).
- [15] T. Gregor, D. Tank, E. Wieschaus, and W. Bialek, Probing the limits to positional information, *Cell* **130**, 153 (2007).
- [16] W. Bialek, Biophysics: Searching for principles, Biophysics: Searching for Principles (2012).
- [17] G. Tkačik, J. O. Dubuis, M. D. Petkova, and T. Gregor, Positional Information, Positional Error, and Readout Precision in Morphogenesis: A Mathematical Framework, *Genetics* **199**, 39 (2014).
- [18] P. Hillenbrand, U. Gerland, and G. Tkačik, Beyond the french flag model: Exploiting spatial and gene regulatory interactions for positional information, *PLoS ONE* **11**, 1 (2016).
- [19] G. Tkačik and T. Gregor, The many bits of positional information, *Development* **148**, dev176065 (2021).
- [20] K. S. Iyer, C. Prabhakara, S. Mayor, and M. Rao, Cellular compartmentalisation and receptor promiscuity as a strategy for accurate and robust inference of position during morphogenesis, *eLife* **12**, e79257 (2023).
- [21] R. A. Blythe and M. R. Evans, Nonequilibrium steady states of matrix-product form: a solver’s guide, *Journal of Physics A: Mathematical and Theoretical* **40**, R333 (2007).
- [22] B. Derrida, M. R. Evans, V. Hakim, and V. Pasquier, Exact solution of a 1d asymmetric exclusion model using a matrix formulation, *Journal of Physics A: Mathematical and General* **26**, 1493 (1993).
- [23] B. Derrida, J. L. Lebowitz, and E. R. Speer, Free energy functional for nonequilibrium systems: An exactly solvable case, *Physical Review Letters* **87**, 150601 (2001).
- [24] B. Derrida, J. L. Lebowitz, and E. R. Speer, Large deviation of the density profile in the steady state of the open symmetric simple exclusion process, *Journal of Statistical Physics* **107**, 599 (2002).
- [25] B. Derrida, Non-equilibrium steady states: fluctuations and large deviations of the density and of the current, *Journal of Statistical Mechanics: Theory and Experiment*, P07023 (2007).
- [26] E. Levine, D. Mukamel, and G. M. Schütz, Zero-range process with open boundaries, *Journal of Statistical Physics* **120**, 759 (2005).
- [27] G. Schütz, Exactly solvable models for many-body systems far from equilibrium (Academic Press, 2001).
- [28] P. Singh and K. Proesmans, Supplementary material for

- “limits to positional information in boundary-driven systems” (2024).
- [29] L. McGough, H. Casademunt, M. c. v. Nikolić, Z. Aridor, M. D. Petkova, T. Gregor, and W. Bialek, Finding the last bits of positional information, [PRX Life](#) **2**, 013016 (2024).
- [30] S. R. d. Groot and P. Mazur, *Non-equilibrium Thermodynamics* (Dover Publications, New York, 1984) (1984).
- [31] S. Sasa, Derivation of hydrodynamics from the hamiltonian description of particle systems, [Physical Review Letters](#) **112**, 100602 (2014).
- [32] M. J. Thompson, C. A. Young, V. Munnamalai, and D. M. Umulis, Early radial positional information in the cochlea is optimized by a precise linear bmp gradient and enhanced by sox2, [Scientific Reports](#) **13**, 8567 (2023).
- [33] K. Vafayi and M. H. Duong, Weakly nonequilibrium properties of a symmetric inclusion process with open boundaries, [Physical Review E](#) **90**, 052143 (2014).
- [34] C. Franceschini, P. Gonçalves, and F. Sau, Symmetric inclusion process with slow boundary: Hydrodynamics and hydrostatics, [Bernoulli](#) **28**, 1340 (2022).
- [35] M. E. Cates and J. Tailleur, Motility-induced phase separation, [Annual Review of Condensed Matter Physics](#) **6**, 219 (2015).
- [36] G. L. Eyink, J. L. Lebowitz, and H. Spohn, Hydrodynamics and fluctuations outside of local equilibrium: Driven diffusive systems, [Journal of Statistical Physics](#) **83**, 385 (1996).

**SUPPLEMENTARY MATERIAL: LIMITS TO POSITIONAL INFORMATION IN BOUNDARY-DRIVEN SYSTEMS**

Prashant Singh and Karel Proesmans  
*Niels Bohr International Academy, Niels Bohr Institute,  
 University of Copenhagen, Blegdamsvej 17, 2100 Copenhagen, Denmark*

In this supplementary note, we will present an extensive derivation of the results which were quoted in the main text of our letter. To begin with, it is useful to recall the mathematical framework of positional information developed in [1]

**I. MATHEMATICAL FRAMEWORK FOR POSITIONAL INFORMATION**

Wolpert's idea is that although cells do not have any direct way to measure their positions, they can still acquire positional information by reading out the local concentration of the signalling morphogen molecules [2]. During the initial stage of development, cells inside an embryo might be distributed in a certain way, and depending on the initial knowledge about their positions, one will have some form of prior probability  $P_i(i)$ . Now if one observes a certain morphogen concentration  $n$ , then the position of a cell can be more accurately specified. However, due to the fact that the cells are in a noisy environment, the position of a cell after measurement is still drawn from a probability distribution  $P(i|n)$  but conditioned on the value  $n$ . Observe that this conditional distribution is always narrower than the prior  $P_i(i)$ , and the degree of this narrowness represents the amount of positional information gained by the cells. For instance, if the distribution  $P(i|n)$  has same flatness as  $P_i(i)$ , then not much information is gained about the position of the cell. On the other hand, if  $P(i|n)$  is highly peaked at some value of  $i$ , then the position of a cell is determined with more precision.

The two distributions  $P_i(i)$  and  $P(i|n)$  are the main ingredients in this framework and the information gained by measuring the concentration  $n$  is given by

$$\mathbb{I}_{n \rightarrow i} = S[P_i(i)] - S[P(i|n)], \quad (\text{S1})$$

where  $S[P_i(i)]$  and  $S[P(i|n)]$  are the entropies associated with distributions  $P_i(i)$  and  $P(i|n)$

$$S[P_i(i)] = - \sum_{i=1}^N P_i(i) \log_2 [P_i(i)], \quad (\text{S2})$$

$$S[P(i|n)] = - \sum_{i=1}^N P(i|n) \log_2 [P(i|n)]. \quad (\text{S3})$$

The fact that  $P(i|n)$  is narrower than  $P_i(i)$  implies that  $S[P(i|n)]$  is smaller than  $S[P_i(i)]$ . Hence  $\mathbb{I}_{n \rightarrow i}$  in Eq. (S1) can take only non-negative values. Moreover, we will assume that  $n$  is a continuous variable. When it takes discrete values, the integration over  $n$  need to be replaced by its summation (same applies to  $i$ ).

Now if we randomly choose a cell, then the morphogen concentration will be distributed as  $P_n(n)$  and taking the average of Eq. (S1) with this distribution gives us

$$\mathcal{I}_{(n,i)}(\{\rho\}) = \int dn P_n(n) [S[P_i(i)] - S[P(i|n)]], \quad (\text{S4})$$

$$= \sum_{i=1}^N \int dn P(i, n) \log_2 \left[ \frac{P(i, n)}{P_i(i)P_n(n)} \right]. \quad (\text{S5})$$

Here  $P(i, n) = P(i|n)P_n(n) = P(n|i)P_i(i)$  stands for the joint distribution of  $n$  and  $i$ . Moreover, we have written positional information as a function of model parameters  $\{\rho\}$  whose precise definition will be given later. Interestingly, the expression in Eq. (S5) emphasizes that the average information is mutual, *i.e.* the information gained about the position of a cell by measuring the morphogen concentration is on average same as the information gained about the morphogen concentration by measuring the position of a cell. We therefore have

$$\mathcal{I}_{(n,i)}(\{\rho\}) = \sum_{i=1}^N P_i(i) [S[P_n(n)] - S[P(n|i)]], \quad (\text{S6})$$

with entropies measured in bits as

$$S[P_n(n)] = - \int dn P_n(n) \log_2 [P_n(n)], \quad (\text{S7})$$

$$S[P(n|i)] = - \int dn P(n|i) \log_2 [P(n|i)]. \quad (\text{S8})$$

In some of our calculations below, Eq. (S6) turns out to be more useful to calculate the positional information.

## II. A PERTURBATIVE APPROACH FOR POSITIONAL INFORMATION IN BOUNDARY-DRIVEN SYSTEMS

In this section, we develop a perturbative approach to obtain the positional information for general boundary driven systems. Let us consider a one-dimensional lattice system consisting of  $N$  ( $\gg 1$ ) sites represented by the index  $i$  with  $1 \leq i \leq N$ . These sites can either accommodate an arbitrary non-negative number of particles (as observed in systems like ZRP or IRW) or can have at most a fixed number of particles (as seen in SSEP). In bulk where  $1 < i < N$ , a particle can jump to either of its neighbouring sites with an arbitrary rate (the rate can also depend on the occupation numbers of these sites). On the other hand, at the two end sites ( $i = 1$  and  $i = N$ ), the system is in contact with two particle reservoirs characterised by the average densities  $\rho_L$  and  $\rho_R$  and chemical potentials  $\mu_L$  and  $\mu_R$ . However, both reservoirs have the same temperature  $T$ . Without any loss of generality, we will take  $\rho_L \geq \rho_R$  and denote the Boltzmann constant by  $k_B$ . Due to the coupling with the reservoirs, we assume that the system eventually reaches a non-equilibrium steady-state.

Our approach relies on the fact that even though there are significant departures from equilibrium in the system as a whole, local regions can still be described, to first order in gradients, by an equilibrium measure with parameters that vary slowly across the system. This *local thermodynamic equilibrium* allows one to identify thermodynamic quantities such as chemical potential locally even in out-of-equilibrium set-ups. With this idea in mind, we now consider a small volume  $v_c$  around the lattice site  $i$  and write the probability distribution to observe a number  $n$  inside this volume as

$$P(n|i) \sim \exp \left[ - \frac{v_c}{k_B T} \left( \mathcal{G}_{\mu_i}(n/v_c) - \mathcal{G}_{\mu_i}(\rho_i) \right) \right], \quad (\text{S9})$$

where  $\mathcal{G}_{\mu_i}(g)$  is given in terms of the Helmholtz free energy  $a(g)$  per unit volume as

$$\mathcal{G}_{\mu_i}(g) = a(g) - \mu_i g \quad \text{and} \quad \mu_i = \left. \frac{\partial a(g)}{\partial g} \right|_{g=\rho_i}. \quad (\text{S10})$$

Here  $\mu_i$  is the local chemical potential which is given in terms of the local average density  $\rho_i = \langle n_i/v_c \rangle$  such that  $\rho_1 = \rho_L$  and  $\rho_N = \rho_R$ . In this description, the microscopic details of the system such as inter-particle interaction, dynamics etc, are captured by the form of  $a(g)$  and the average density  $\rho_i$ . For models studied in the letter, the derivation of  $a(g)$  is given in section IX.

Although the precise form of  $\rho_i$  depends on the specific model, it turns out useful to expand  $\rho_i$  as a series in  $\Delta\rho = (\rho_L - \rho_R)/2$  as

$$\rho_i = \bar{\rho} + \left( 1 - \frac{2i}{N} \right) \Delta\rho + \sum_{k=2}^{\infty} \mathcal{L}_k(i, \bar{\rho}) \Delta\rho^k, \quad (\text{S11})$$

where  $\bar{\rho} = (\rho_L + \rho_R)/2$ . For computational convenience, we have written the  $k = 1$  term separately in the above expression and taken it to be  $\mathcal{L}_1(i, \bar{\rho}) = \left( 1 - \frac{2i}{N} \right)$ . This form is sensible because the average density should remain invariant under the transformation  $\rho_L \leftrightarrow \rho_R$  and  $i \rightarrow (N - i)$ . By the same symmetry argument, we must also have  $\mathcal{L}_k(i, \bar{\rho}) = (-1)^k \mathcal{L}_k(N - i, \bar{\rho})$  for all values of  $k$ . Apart from this symmetry, we do not make any assumption on  $\mathcal{L}_k(i, \bar{\rho})$  and their specific forms will depend on the model.

Using the expansion in Eq. (S11), the local chemical potential  $\mu_i$  and the free energy in Eq. (S10) can also be

expanded in  $\Delta\rho$  as

$$\mu_i = \bar{\mu} + \sum_{k=1}^{\infty} \frac{a_{k+1}(\bar{\rho})}{k!} [\mathcal{K}(i, \bar{\rho})]^k, \quad (\text{S12})$$

$$\mathcal{G}_{\mu_i}(g) = \mathcal{G}_{\bar{\mu}}(g) - g \sum_{k=1}^{\infty} \frac{a_{k+1}(\bar{\rho})}{k!} [\mathcal{K}(i, \bar{\rho})]^k, \quad (\text{S13})$$

$$\mathcal{G}_{\mu_i}(\rho_i) = \mathcal{G}_{\bar{\mu}}(\bar{\rho}) - \bar{\rho} \sum_{k=1}^{\infty} \frac{a_{k+1}(\bar{\rho})}{k!} [\mathcal{K}(i, \bar{\rho})]^k - \sum_{k=2}^{\infty} \frac{(k-1)a_k(\bar{\rho})}{k!} [\mathcal{K}(i, \bar{\rho})]^k, \quad (\text{S14})$$

where we use the notation

$$\bar{\mu} = \frac{\partial a(\bar{\rho})}{\partial \bar{\rho}}, \quad a_k(\bar{\rho}) = \frac{d^k a(\bar{\rho})}{d\bar{\rho}^k}, \quad \mathcal{K}(i, \bar{\rho}) = \rho_i - \bar{\rho}. \quad (\text{S15})$$

Plugging the expansions in Eq. (S9) yields

$$P(n|i) = P_{\text{eq}}(n) \exp \left[ \frac{v_c}{k_B T} (n/v_c - \bar{\rho}) \sum_{k=1}^{\infty} \frac{a_{k+1}(\bar{\rho})}{k!} [\mathcal{K}(i, \bar{\rho})]^k - \frac{v_c}{k_B T} \sum_{k=2}^{\infty} \frac{(k-1)a_k(\bar{\rho})}{k!} [\mathcal{K}(i, \bar{\rho})]^k \right], \quad (\text{S16})$$

where  $P_{\text{eq}}(n) \sim e^{-\frac{v_c}{k_B T} (\mathcal{G}_{\bar{\mu}}(n/v_c) - \mathcal{G}_{\bar{\mu}}(\bar{\rho}))}$  is the equilibrium measure with average density  $\bar{\rho}$  and chemical potential  $\bar{\mu}$ . The idea now is to use this series expansion in Eq. (S5) to obtain a perturbation expansion for the positional information. Let us calculate the first term in the expansion.

#### A. First term

It turns out, as also demonstrated later, that the first term is of the order  $\sim \Delta\rho^2$ . Hence, we include all terms up to this order in the density expansion in Eq. (S11) and truncate  $\mathcal{K}(i, \bar{\rho})$  as

$$\mathcal{K}(i, \bar{\rho}) \simeq \mathcal{L}_1(i, \bar{\rho}) \Delta\rho + \mathcal{L}_2(i, \bar{\rho}) \Delta\rho^2, \quad \text{with } \mathcal{L}_1(i, \bar{\rho}) = \left(1 - \frac{2i}{N}\right) \quad (\text{S17})$$

From Eq. (S16), it then follows

$$P(n|i) \simeq P_{\text{eq}}(n) [1 + f_1(i, n)\Delta\rho + f_2(i, n)\Delta\rho^2], \quad (\text{S18})$$

with two functions  $f_1(i, n)$  and  $f_2(i, n)$  defined as

$$f_1(i, n) = \frac{v_c}{k_B T} \mathcal{L}_1(i, \bar{\rho}) a_2(\bar{\rho}) (n/v_c - \bar{\rho}), \quad (\text{S19})$$

$$f_2(i, n) = \frac{v_c}{2k_B T} \left\{ -a_2(\bar{\rho}) \mathcal{L}_1(i, \bar{\rho})^2 + \frac{v_c}{k_B T} a_2(\bar{\rho})^2 \mathcal{L}_1(i, \bar{\rho})^2 (n/v_c - \bar{\rho})^2 + \left(2a_2(\bar{\rho}) \mathcal{L}_2(i, \bar{\rho}) + a_3(\bar{\rho}) \mathcal{L}_1(i, \bar{\rho})^2\right) (n/v_c - \bar{\rho}) \right\}. \quad (\text{S20})$$

For a given prior  $P_i(i)$ , the joint distribution  $P(i, n)$  can be written using Bayes' theorem as  $P(i, n) = P(n|i)P_i(i)$ . Moreover, the marginal distribution  $P_n(n)$  can be calculated to be

$$P_n(n) = \sum_{i=1}^N P(n|i) P_i(i), \quad (\text{S21})$$

$$\simeq P_{\text{eq}}(n) [1 + \langle f_1(i, n) \rangle_i \Delta\rho + \langle f_2(i, n) \rangle_i \Delta\rho^2], \quad (\text{S22})$$

with the notation  $\langle f_1(i, n) \rangle_i = \sum_{i=1}^N P_i(i) f_1(i, n)$  and same for  $\langle f_2(i, n) \rangle_i$ . We now have all quantities required to compute the positional information in Eq. (S5). Inserting these distributions, the first term in  $\mathcal{I}_{(n,i)}(\bar{\rho}, \Delta\rho)$  can be written as

$$\mathcal{I}_{(n,i)}(\bar{\rho}, \Delta\rho) \approx \frac{2v_c^2 \Delta\rho^2 a_2(\bar{\rho})^2 \sigma_2(\bar{\rho})}{(k_B T)^2 \ln 2} \left[ \left\langle \left( \frac{i}{N} \right)^2 \right\rangle_i - \left\langle \left( \frac{i}{N} \right) \right\rangle_i^2 \right], \quad (\text{S23})$$

$$\approx \frac{2\Delta\rho^2}{\ln 2 \sigma_2(\bar{\rho})} \left[ \left\langle \left( \frac{i}{N} \right)^2 \right\rangle_i - \left\langle \left( \frac{i}{N} \right) \right\rangle_i^2 \right], \quad (\text{S24})$$

where  $\sigma_k(\bar{\rho}) = \langle (n/v_c - \bar{\rho})^k \rangle_{\text{eq}}$  denotes the  $k$ -th central moment. In writing Eq. (S24), we have used the fluctuation-response relation  $a_2(\bar{\rho}) = k_B T / \sigma_2(\bar{\rho}) v_c$ . For completeness, the proof of this relation is provided in Section VIII. To sum up, we have derived the first term in the series expansion of  $\mathcal{I}_{(n,i)}(\bar{\rho}, \Delta\rho)$  for any prior in terms of the second central moment of the density at equilibrium.

### B. Second term

In order to obtain the second order term in the expansion, we have to consider higher order terms in the expansion of density in Eq. (S11). The second term is of the order  $\sim \Delta\rho^4$  and we therefore take

$$\mathcal{K}(i, \bar{\rho}) \simeq \left(1 - \frac{2i}{N}\right) \Delta\rho + \mathcal{L}_2(i, \bar{\rho}) \Delta\rho^2 + \mathcal{L}_3(i, \bar{\rho}) \Delta\rho^3 + \mathcal{L}_4(i, \bar{\rho}) \Delta\rho^4. \quad (\text{S25})$$

We now proceed exactly as before but keeping terms up to order  $\sim \Delta\rho^4$  in the analysis. This gives us the higher order terms for  $\mathcal{I}_{(n,i)}(\bar{\rho}, \Delta\rho)$ . For the case of flat prior  $P_i(i) = 1/N$ , the second order term is obtained to be

$$\begin{aligned} \mathcal{I}_{(n,i)}(\bar{\rho}, \Delta\rho) \simeq & \frac{\Delta\rho^2}{6 \ln 2 \sigma_2(\bar{\rho})} + \frac{8 v_c \Delta\rho^4}{45 k_B T \ln 2} \left[ \frac{4a_2(\bar{\rho})a_4(\bar{\rho}) - 5(a_3(\bar{\rho})^2 + a_2(\bar{\rho})^3)}{32a_2(\bar{\rho})} + \frac{45a_3(\bar{\rho})}{16N} \sum_{i=1}^N \mathcal{L}_2(i, \bar{\rho}) \left(\frac{4i^2}{N^2} - 1\right) \right. \\ & \left. - \frac{45}{16} a_2(\bar{\rho}) \left\{ \left(N^{-1} \sum_{i=1}^N \mathcal{L}_2(i, \bar{\rho})\right)^2 - N^{-1} \sum_{i=1}^N \mathcal{L}_2(i, \bar{\rho})^2 - 2N^{-1} \sum_{i=1}^N \mathcal{L}_3(i, \bar{\rho}) \mathcal{L}_1(i, \bar{\rho}) \right\} \right]. \quad (\text{S26}) \end{aligned}$$

For later comparison, it is useful to write this expression in terms of the  $\sigma_k(\bar{\rho})$ . To achieve this, we use the following set of relations

$$\frac{v_c a_2(\bar{\rho})}{k_B T} = \frac{1}{\sigma_2(\bar{\rho})}, \quad \frac{v_c a_3(\bar{\rho})}{k_B T} = -\frac{\sigma_3(\bar{\rho})}{\sigma_2(\bar{\rho})^3}, \quad \frac{v_c a_4(\bar{\rho})}{k_B T} = -\frac{\sigma_4(\bar{\rho})}{\sigma_2(\bar{\rho})^4} + \frac{3}{\sigma_2(\bar{\rho})^5} [\sigma_3(\bar{\rho})^2 + \sigma_2(\bar{\rho})^3], \quad (\text{S27})$$

which have been derived in Section VIII. The above expression now becomes

$$\begin{aligned} \mathcal{I}_{(n,i)}(\bar{\rho}, \Delta\rho) \approx & \frac{\Delta\rho^2}{6 \ln 2 \sigma_2(\bar{\rho})} + \frac{8 \Delta\rho^4}{45 \ln 2 \sigma_2(\bar{\rho})} \left[ \frac{7(\sigma_3(\bar{\rho})^2 + \sigma_2(\bar{\rho})^3) - 4\sigma_2(\bar{\rho})\sigma_4(\bar{\rho})}{32 \sigma_2(\bar{\rho})^4} + \frac{45\sigma_3(\bar{\rho})}{16\sigma_2(\bar{\rho})^2 N} \sum_{i=1}^N \mathcal{L}_2(i, \bar{\rho}) \left(\frac{4i^2}{N^2} - 1\right) \right. \\ & \left. - \frac{45}{16} \left\{ \left(N^{-1} \sum_{i=1}^N \mathcal{L}_2(i, \bar{\rho})\right)^2 - N^{-1} \sum_{i=1}^N \mathcal{L}_2(i, \bar{\rho})^2 - 2N^{-1} \sum_{i=1}^N \mathcal{L}_3(i, \bar{\rho}) \mathcal{L}_1(i, \bar{\rho}) \right\} \right]. \quad (\text{S28}) \end{aligned}$$

This gives the first two terms in the series expansion of the positional information. One can also obtain the higher order terms in the same way. In summary, we have developed a perturbative approach to calculate  $\mathcal{I}_{(n,i)}(\bar{\rho}, \Delta\rho)$  for a general boundary-driven system. Our approach relies on the local equilibrium assumption and requires only the knowledge of the average density  $\rho_i$ . Positional information is then obtained as an expansion in  $\Delta\rho$  with coefficients depending on the equilibrium central moments of the density (or equivalently the derivatives of the free energy).

### C. Connection of $\mathcal{I}_{(n,i)}(\bar{\rho}, \Delta\rho)$ with the chemical potential difference for a general $P_i(i)$

Having developed a methodology to compute positional information, we are now in a position to establish its connection with the chemical potential difference driving the system,  $\Delta\mu = \mu_L - \mu_R$ . Following Eq. (S10), this can be written as

$$\Delta\mu = a_1(\bar{\rho} + \Delta\rho) - a_1(\bar{\rho} - \Delta\rho) \simeq \frac{2k_B T \Delta\rho}{v_c \sigma_2(\bar{\rho})}. \quad (\text{S29})$$

Combining this with the expression of  $\mathcal{I}_{(n,i)}(\bar{\rho}, \Delta\rho)$  in Eq. (S24), we obtain for the leading order in  $\Delta\rho$

$$\mathcal{I}_{(n,i)}(\bar{\rho}, \Delta\rho) \approx \frac{\Delta\mu v_c \Delta\rho}{k_B T \ln 2} \left[ \left\langle \left(\frac{i}{N}\right)^2 \right\rangle_i - \left\langle \left(\frac{i}{N}\right) \right\rangle_i^2 \right]. \quad (\text{S30})$$

This relation quantitatively gives the link between the positional information and non-equilibrium nature of the system for a given prior. At least with only the first term in  $\mathcal{I}_{(n,i)}(\bar{\rho}, \Delta\rho)$  and  $\Delta\mu$ , Eq. (S30) tells us how positional information increases on increasing the non-equilibrium drive.

We are now interested in optimising Eq. (S30) with respect to  $P_i(i)$ . First recall that the index  $i$  can take only positive integer values and is bounded as  $1 \leq i \leq N$ . This means

$$\frac{i}{N} \leq 1 \implies \left(\frac{i}{N}\right)^2 \leq \left(\frac{i}{N}\right). \quad (\text{S31})$$

Averaging both sides

$$\left\langle \left(\frac{i}{N}\right)^2 \right\rangle_i \leq \left\langle \frac{i}{N} \right\rangle_i \quad (\text{S32})$$

Using this in Eq. (S30), one can write the bound

$$\mathcal{I}_{(n,i)}(\bar{\rho}, \Delta\rho) \leq \frac{\Delta\mu v_c \Delta\rho}{k_B T \ln 2} \left[ \left\langle \frac{i}{N} \right\rangle_i - \left\langle \frac{i}{N} \right\rangle_i^2 \right]. \quad (\text{S33})$$

Let us find the bound on the term inside [...]. Using the following relation

$$\left( \left\langle \frac{i}{N} \right\rangle_i - \frac{1}{2} \right)^2 \geq 0, \implies \left[ \left\langle \frac{i}{N} \right\rangle_i - \left\langle \frac{i}{N} \right\rangle_i^2 \right] \leq \frac{1}{4} \quad (\text{S34})$$

in the above inequality, we obtain

$$\mathcal{I}_{(n,i)}(\bar{\rho}, \Delta\rho) \leq \frac{\Delta\mu v_c \Delta\rho}{4k_B T \ln 2}. \quad (\text{S35})$$

This gives a universal bound to the near-equilibrium positional information that is valid for for any boundary-driven systems with arbitrary choice of prior.

Beyond linear response regime, writing any universal relation is difficult due to the dependence of higher-order terms in positional information on the specific model, as illustrated in Eq. (S28). In absence of a general formulation, we have studied several solvable boundary-driven systems. For each of these models, we find that the upper bound (S35) is valid even in the far-from equilibrium conditions and we obtain a fundamental limit on the positional information in terms of the system's distance from the equilibrium.

For the case of a flat prior, our analysis on these solvable models reveal that there exists a tighter bound to the positional information compared to the one in (S35)

$$\mathcal{I}_{(n,i)}(\bar{\rho}, \Delta\rho) \leq \frac{\Delta\mu v_c \Delta\rho}{12 k_B T \ln 2}. \quad (\text{S36})$$

This bound is saturated if the system is close to equilibrium. This can be verified by plugging the variance

$$\left[ \left\langle \left(\frac{i}{N}\right)^2 \right\rangle_i - \left\langle \frac{i}{N} \right\rangle_i^2 \right] \simeq \frac{1}{12}, \text{ for large } N \quad (\text{S37})$$

in our general expression in Eq. (S30). In what follows, we will first look at the flat prior case and demonstrate numerically the upper bound (S36) for different toy models when they are arbitrarily from from the equilibrium. After that, we will investigate how positional information varies for different priors in section VI and test the other bound (S35) for these models. Below, we first look at SSEP followed by a number of other models. In rest of our analysis, we will set  $k_B T = 1$  and  $v_c = 1$  for simplicity.

### III. POSITIONAL INFORMATION FOR THE BOUNDARY-DRIVEN SSEP

One of the models that we discussed in the main text is the open symmetric simple exclusion process (SSEP). The model consists of  $N$  lattice sites in one dimension represented by the index  $i$  that runs from 1 to  $N$ . Each lattice

site can either be vacant ( $n_i = 0$ ) or occupied by a single particle ( $n_i = 1$ ). The dynamics of the particles are as follows: Within the bulk, where  $1 < i < N$ , a particle can jump to either of its neighbouring sites with a rate  $p$ , provided that these neighbouring sites are empty. On the other hand, the two boundary sites ( $i = 1$  and  $i = N$ ) are in contact with two different particle reservoirs, and their dynamics are modified accordingly. At  $i = 1$ , a particle can be added (removed) with a rate  $\alpha_L$  ( $\beta_L$ ) if the site is vacant (occupied). Conversely, at  $i = N$ , a particle can be added (removed) with a rate  $\alpha_R$  ( $\beta_R$ ) if it is vacant (occupied). At any small time interval  $[t, t + dt]$ , the occupancy variable  $n_i(t)$  for each lattice site evolves according to the following update rule [3, 4]

$$n_i(t + \Delta t) - n_i(t) = \begin{cases} n_{i+1}(t), & \text{w.p. } [1 - n_i(t)] p \Delta t, \\ n_{i-1}(t), & \text{w.p. } [1 - n_i(t)] p \Delta t, \\ -n_i(t), & \text{w.p. } [1 - n_{i+1}(t)] p \Delta t, \\ -n_i(t), & \text{w.p. } [1 - n_{i-1}(t)] p \Delta t, \\ 0, & \text{otherwise,} \end{cases}, \quad \text{for } i \neq 1, \quad i \neq N \quad (\text{S38})$$

$$n_1(t + \Delta t) - n_1(t) = \begin{cases} -n_1(t), & \text{w.p. } [1 - n_2(t)] p \Delta t, \\ n_2(t), & \text{w.p. } [1 - n_1(t)] p \Delta t, \\ 1, & \text{w.p. } [1 - n_1(t)] \alpha_L \Delta t, \\ -1, & \text{w.p. } n_1(t) \beta_L \Delta t, \\ 0, & \text{otherwise,} \end{cases} \quad (\text{S39})$$

$$n_N(t + \Delta t) - n_N(t) = \begin{cases} -n_N(t), & \text{w.p. } [1 - n_{N-1}(t)] p \Delta t, \\ n_{N-1}(t), & \text{w.p. } [1 - n_N(t)] p \Delta t, \\ 1, & \text{w.p. } [1 - n_N(t)] \alpha_R \Delta t, \\ -1, & \text{w.p. } n_N(t) \beta_R \Delta t, \\ 0, & \text{otherwise,} \end{cases} \quad (\text{S40})$$

where ‘‘w.p’’ is the short-hand notation for ‘‘with probability’’. Our aim is to calculate the positional information for this model. As evident from its definition, it is then necessary to compute the conditional probability  $P(n|i)$  of having  $n$  particles at  $i$ -th site. Later, we show that this probability can be expressed in terms of the mean density  $\rho_i(t) = \langle n_i(t) \rangle$ . Therefore, in what follows, we will first calculate  $\rho_i(t)$ .

### A. Average density $\rho_i(t) = \langle n_i(t) \rangle$

From the update rules written above, one can write the differential equations for  $\rho_i(t)$  as

$$\frac{\partial \rho_i(t)}{\partial t} = p [\rho_{i+1}(t) + \rho_{i-1}(t) - 2\rho_i(t)], \quad (\text{for } i \neq 1, \quad i \neq N) \quad (\text{S41})$$

$$\frac{\partial \rho_1(t)}{\partial t} = \alpha_L - (p + \alpha_L + \beta_L)\rho_1(t) + p \rho_2(t), \quad (\text{S42})$$

$$\frac{\partial \rho_N(t)}{\partial t} = \alpha_R - (p + \alpha_R + \beta_R)\rho_N(t) + p \rho_{N-1}(t). \quad (\text{S43})$$

Since we are interested in the steady-state properties, we replace the time derivatives on the left hand sides of these equations by zero and obtain the solution as

$$\rho_i(t \rightarrow \infty) = \mathcal{A} + (i - 1) \mathcal{B}, \quad (\text{S44})$$

$$\text{with } \mathcal{A} = \frac{\alpha_L (\alpha_R + \beta_R) (N - 1) + p (\alpha_L + \alpha_R)}{(\alpha_L + \beta_L) (\alpha_R + \beta_R) (N - 1) + p (\alpha_L + \beta_L + \alpha_R + \beta_R)}, \quad (\text{S45})$$

$$\mathcal{B} = \frac{\alpha_R \beta_L - \alpha_L \beta_R}{(\alpha_L + \beta_L) (\alpha_R + \beta_R) (N - 1)}. \quad (\text{S46})$$

For large  $N$ , one can rewrite this expression as

$$\rho_i \simeq \rho_L - (\rho_L - \rho_R) \frac{i}{N}, \quad \text{with } \rho_L = \frac{\alpha_L}{\alpha_L + \beta_L}, \quad \rho_R = \frac{\alpha_R}{\alpha_R + \beta_R}. \quad (\text{S47})$$

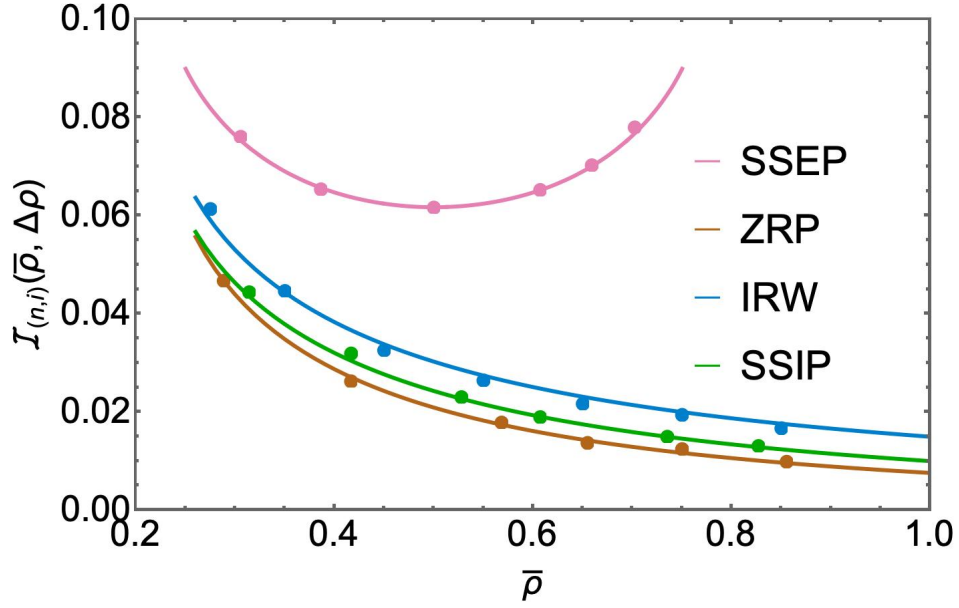


FIG. S1. Plot of the positional information as a function of  $\bar{\rho}$  for four different boundary-driven processes and its comparison with the numerical simulations. In each case, solid lines illustrate the analytical expression, while symbols denote simulation data. We have fixed the bias to  $\Delta\rho = 0.25$  and chosen the flat prior.

We have used  $\rho_L$  and  $\rho_R$  to represent the average densities of the left and the right reservoir respectively and are expressed in terms of the parameters of our model. Furthermore, the approximate equality in Eq. (S48) is used to indicate that we are working in the large  $N$  limit. Finally, we express density in terms of the variables  $\bar{\rho} = (\rho_L + \rho_R)/2$  and  $\Delta\rho = (\rho_L - \rho_R)/2$

$$\rho_i \simeq \bar{\rho} + \left(1 - \frac{2i}{N}\right) \Delta\rho, \quad (\text{S48})$$

and utilize this form to derive the positional information.

### B. Positional information

In order to obtain the positional information, we will use its definition in Eq. (S6) and calculate the entropies  $S[P(n|i)]$  and  $S[P_n(n)]$ . Recall that  $n_i$  is a binary variable that can take values either 0 or 1 depending on whether the site is vacant or occupied. We therefore have  $\rho_i = 1 \times P(n = 1|i) + 0 \times P(n = 0|i) = P(n = 1|i)$ . The complementary probability will then simply be  $P(n = 0|i) = 1 - \rho_i$ .

$$P(n = 1|i) = \rho_i = \bar{\rho} + \left(1 - \frac{2i}{N}\right) \Delta\rho, \quad (\text{S49})$$

$$P(n = 0|i) = 1 - \rho_i = 1 - \bar{\rho} - \left(1 - \frac{2i}{N}\right) \Delta\rho. \quad (\text{S50})$$

From these, we get

$$S[P(n|i)] = - \sum_{n=\{0,1\}} P(n|i) \log_2[P(n|i)], \quad (\text{S51})$$

$$\begin{aligned} &= - \left[ \bar{\rho} + \left(1 - \frac{2i}{N}\right) \Delta\rho \right] \log_2 \left[ \bar{\rho} + \left(1 - \frac{2i}{N}\right) \Delta\rho \right] \\ &\quad - \left[ 1 - \bar{\rho} - \left(1 - \frac{2i}{N}\right) \Delta\rho \right] \log_2 \left[ 1 - \bar{\rho} - \left(1 - \frac{2i}{N}\right) \Delta\rho \right]. \end{aligned} \quad (\text{S52})$$

For the average information in Eq. (S6), we also have to perform averaging of  $S[P(n|i)]$  over the prior distribution  $P_i(i)$  which we have chosen to be uniform. This yields

$$\langle S[P(n|i)] \rangle_i = \sum_{i=1}^{\infty} P_i(i) S[P(n|i)] = \frac{1}{N} \sum_{i=1}^{\infty} S[P(n|i)]$$

Performing this summation turns out to be difficult. We therefore introduce a change of variable  $x = i/N$  and take  $N \rightarrow \infty$ . One can then use the transformation  $1/N \sum_{i=1}^N \rightarrow \int_0^1 dx$  and obtain

$$\begin{aligned} \langle S[P(n|i)] \rangle_i &= - \int_0^1 dx \left[ [\bar{\rho} + (1-2x)\Delta\rho] \log_2 [\bar{\rho} + (1-2x)\Delta\rho] + [1-\bar{\rho} - (1-2x)\Delta\rho] \log_2 [1-\bar{\rho} - (1-2x)\Delta\rho] \right], \\ &= - \frac{1}{\ln 16 (\Delta\rho)} \left[ (\bar{\rho} + \Delta\rho)^2 \ln (\bar{\rho} + \Delta\rho) - (\bar{\rho} - \Delta\rho)^2 \ln (\bar{\rho} - \Delta\rho) - 2\Delta\rho + (1-\bar{\rho} + \Delta\rho)^2 \ln (1-\bar{\rho} + \Delta\rho) \right. \\ &\quad \left. - (1-\bar{\rho} - \Delta\rho)^2 \ln (1-\bar{\rho} - \Delta\rho) \right]. \end{aligned} \quad (\text{S53})$$

We next compute the other entropy,  $S[P_n(n)]$ , in the definition of  $\mathcal{I}_{(n,i)}(\bar{\rho}, \Delta\rho)$ . We can write  $P_n(n)$  by summing over  $i$  in the joint probability  $P(n, i) = P(n|i)$  and then using Eqs. (S49) and (S50) for  $P(n|i)$ . This gives

$$P_n(n) = \frac{1}{N} \sum_{i=1}^N P(n|i) = \bar{\rho} \delta_{n,1} + (1-\bar{\rho}) \delta_{n,0}. \quad (\text{S54})$$

Here  $\delta_{n,1}$  is the Kronecker delta which takes value one if  $n = 1$  and zero otherwise (similarly for  $\delta_{n,0}$ ). Using this expression above, we find

$$S[P_n(n)] = - \sum_{\{n=0,1\}} P_n(n) \log_2 [P_n(n)] = -\bar{\rho} \log_2 \bar{\rho} - (1-\bar{\rho}) \log_2 (1-\bar{\rho}). \quad (\text{S55})$$

We now have all quantities essential for calculating the positional information. Substituting Eqs. (S53) and (S55) in Eq. (S6), the final expression is

$$\mathcal{I}_{(n,i)}(\bar{\rho}, \Delta\rho) = \frac{1}{\ln 16 \Delta\rho} \left[ \mathcal{Y}(\bar{\rho}, \Delta\rho) + \mathcal{Y}(1-\bar{\rho}, \Delta\rho) - 2\Delta\rho \right] - (1-\bar{\rho}) \log_2 (1-\bar{\rho}) - \bar{\rho} \log_2 \bar{\rho}, \quad (\text{S56})$$

$$\text{where } \mathcal{Y}(\bar{\rho}, \Delta\rho) = (\bar{\rho} + \Delta\rho)^2 \ln (\bar{\rho} + \Delta\rho) - (\bar{\rho} - \Delta\rho)^2 \ln (\bar{\rho} - \Delta\rho). \quad (\text{S57})$$

This result has been quoted in the main text. Eq. (S56) is also consistent with our general result in Eq. (S28) in the  $\Delta\rho \rightarrow 0$  limit. In Figure S1, we have plotted  $\mathcal{I}_{(n,i)}(\bar{\rho}, \Delta\rho)$  as a function of  $\bar{\rho}$  and compared it with numerical simulations. We see an excellent agreement between our theoretical formula and the numerics. Notice that for a given  $\Delta\rho$ ,  $\bar{\rho}$  can vary between  $\Delta\rho$  and  $(1-\Delta\rho)$ . Within this range, we find that the positional information for SSEP changes in a non-monotonic manner with  $\bar{\rho}$ . To understand this heuristically, let us see what happens when  $\bar{\rho} \rightarrow (1-\Delta\rho)$  or equivalently  $\rho_L \rightarrow 1$ . In terms of the jump rates, this means that  $\alpha_L \gg \beta_L$  and sites near the left boundary are more likely to be occupied with particles than those near the right boundary. Hence, if we pick a site randomly but is occupied by a particle, it is more likely to be closer to the left boundary than the right one. From the probabilistic perspective, this would imply that the distribution  $P(i|n=1)$  is sharply peaked at  $i=1$ , while the complementary probability  $P(i|n=0)$  peaks at  $i=N$ . The resulting entropy  $\langle S[P(i|n)] \rangle_n$  associated with these peaked distributions, as expressed in Eq. (S1), is small which leads to a larger value of  $\mathcal{I}_{(n,i)}(\bar{\rho}, \Delta\rho)$ . Similarly, for  $\bar{\rho} \rightarrow \Delta\rho$ , one can argue that the probabilities  $P(i|n=1)$  and  $P(i|n=0)$  are narrow functions of  $i$  which again give large  $\mathcal{I}_{(n,i)}(\bar{\rho}, \Delta\rho)$ . In between these large values,  $P(i|n=1)$  and  $P(i|n=0)$  are broadest at some  $\bar{\rho}$  for which the entropy  $\langle S[P(i|n)] \rangle_n$  is highest. This in turn leads to the smallest positional information via Eq. (S1).

### C. Upper bound on $\mathcal{I}_{(n,i)}(\bar{\rho}, \Delta\rho)$

We will now use the derived expression of  $\mathcal{I}_{(n,i)}(\bar{\rho}, \Delta\rho)$  to prove the upper bound in (S36). Observe that the chemical potential difference  $\Delta\mu$  is expressed in terms of the first derivative of the associated free energy in Eq. (S29). To obtain this, we use the fluctuation-response relation in Eq. (S27) as

$$a_2(\bar{\rho}) = \frac{1}{\sigma_2(\bar{\rho})} = \frac{1}{\bar{\rho}(1-\bar{\rho})}, \implies a_1(\bar{\rho}) = \ln \left( \frac{\bar{\rho}}{1-\bar{\rho}} \right). \quad (\text{S58})$$

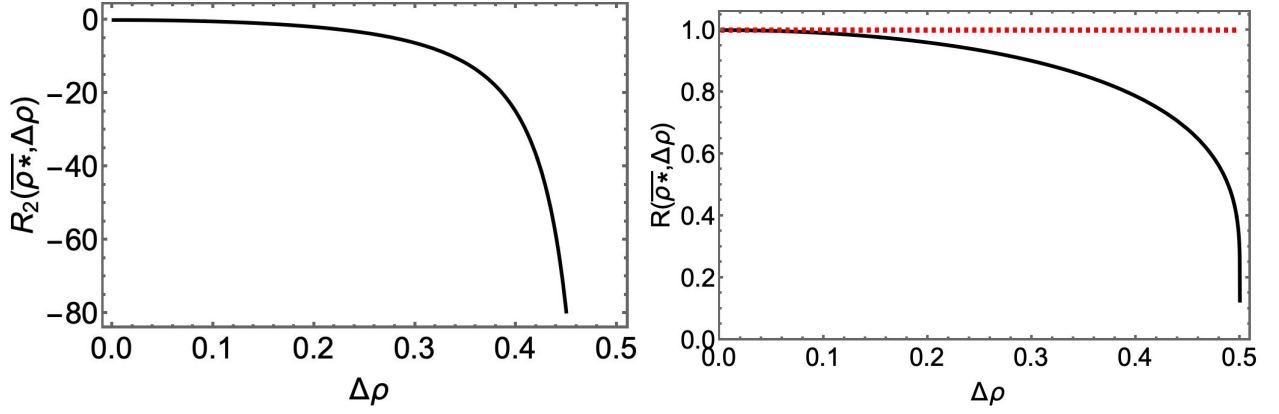


FIG. S2. *Left panel:* Plot of the second derivative  $R_2(\bar{\rho}^*, \Delta\rho) = \left. \frac{\partial^2 R(\bar{\rho}, \Delta\rho)}{\partial \bar{\rho}^2} \right|_{\bar{\rho}=\bar{\rho}^*}$  where  $\bar{\rho}^* = 1/2$ . For all  $\Delta\rho$ , the second derivative takes only negative values. *Right panel:* Illustration of  $R(\bar{\rho}^*, \Delta\rho)$  in Eq. (S62) as a function of  $\Delta\rho$ . The solid black line shows the plot while red dashed line indicates that  $R(\bar{\rho}^*, \Delta\rho)$  is always bounded by the value one.

where  $\sigma_2(\bar{\rho}) = \bar{\rho}(1 - \bar{\rho})$  follows from Eqs. (S49) and (S50) with  $\Delta\rho = 0$  and  $k_B T = 1$  is assumed. Using Eq. (S29), we now get

$$\Delta\mu = \ln\left(\frac{\bar{\rho} + \Delta\rho}{1 - \bar{\rho} - \Delta\rho}\right) - \ln\left(\frac{\bar{\rho} - \Delta\rho}{1 - \bar{\rho} + \Delta\rho}\right). \quad (\text{S59})$$

To derive the bound (S36), it is useful to define a ratio  $R(\bar{\rho}, \Delta\rho)$  as

$$R(\bar{\rho}, \Delta\rho) = \frac{12 \ln 2 \mathcal{I}_{(n,i)}(\bar{\rho}, \Delta\rho)}{\Delta\mu \Delta\rho}. \quad (\text{S60})$$

We are interested in finding the maximum value of this ratio. Below we show that this maximum value turns out to be one thereby proving the upper bound. Proceeding ahead, we take the first derivative of  $R(\bar{\rho}, \Delta\rho)$  with respect to  $\bar{\rho}$  for fixed  $\Delta\rho$

$$\frac{\partial R(\bar{\rho}, \Delta\rho)}{\partial \bar{\rho}} = R(\bar{\rho}, \Delta\rho) \left[ \frac{1}{\mathcal{I}_{(n,i)}(\bar{\rho}, \Delta\rho)} \frac{\partial \mathcal{I}_{(n,i)}(\bar{\rho}, \Delta\rho)}{\partial \bar{\rho}} - \frac{1}{\Delta\mu} \frac{\partial \Delta\mu}{\partial \bar{\rho}} \right], \quad (\text{S61})$$

and setting it to zero, we find the condition for optimality as  $\bar{\rho}^* = 1/2$ . Moreover, the second derivative of  $R(\bar{\rho}, \Delta\rho)$  at  $\bar{\rho}^*$  is always negative indicating that the extremum is a maxima. This is illustrated in the left panel of Figure S2. Therefore, we obtain

$$\begin{aligned} R(\bar{\rho}, \Delta\rho) &\leq R\left(\bar{\rho}^* = \frac{1}{2}, \Delta\rho\right), \\ &= \frac{3}{2\Delta\rho^2} \frac{(1 + 4\Delta\rho^2) \text{Arctanh}(2\Delta\rho) - 2\Delta\rho + 2\Delta\rho \ln(1 - 4\Delta\rho^2)}{\ln(1 + 2\Delta\rho) - \ln(1 - 2\Delta\rho)}. \end{aligned} \quad (\text{S62})$$

Plotting this expression in Figure S2 (right panel), we find that the value of  $R(\bar{\rho}^*, \Delta\rho)$  is always upper bounded by one. From our analysis above, this translates to  $R(\bar{\rho}, \Delta\rho) \leq 1$  and we finally get

$$\mathcal{I}_{(n,i)}(\bar{\rho}, \Delta\rho) \leq \frac{\Delta\mu \Delta\rho}{12 \ln 2}. \quad (\text{S63})$$

Hence for SSEP, we have rigorously derived that the bound (S36) is valid. Moreover, this upper bound turns into an equality in the near-equilibrium regime. To see this, we observe that for  $\Delta\rho \ll \bar{\rho}$  and  $\Delta\rho \ll (1 - \bar{\rho})$ , one can expand  $\mathcal{I}_{(n,i)}(\bar{\rho}, \Delta\rho)$  in Eq. (S56) to obtain

$$\mathcal{I}_{(n,i)}(\bar{\rho}, \Delta\rho) \simeq \frac{\Delta\rho^2}{6 \bar{\rho}(1 - \bar{\rho}) \ln 2} + \mathcal{O}(\Delta\rho^4). \quad (\text{S64})$$

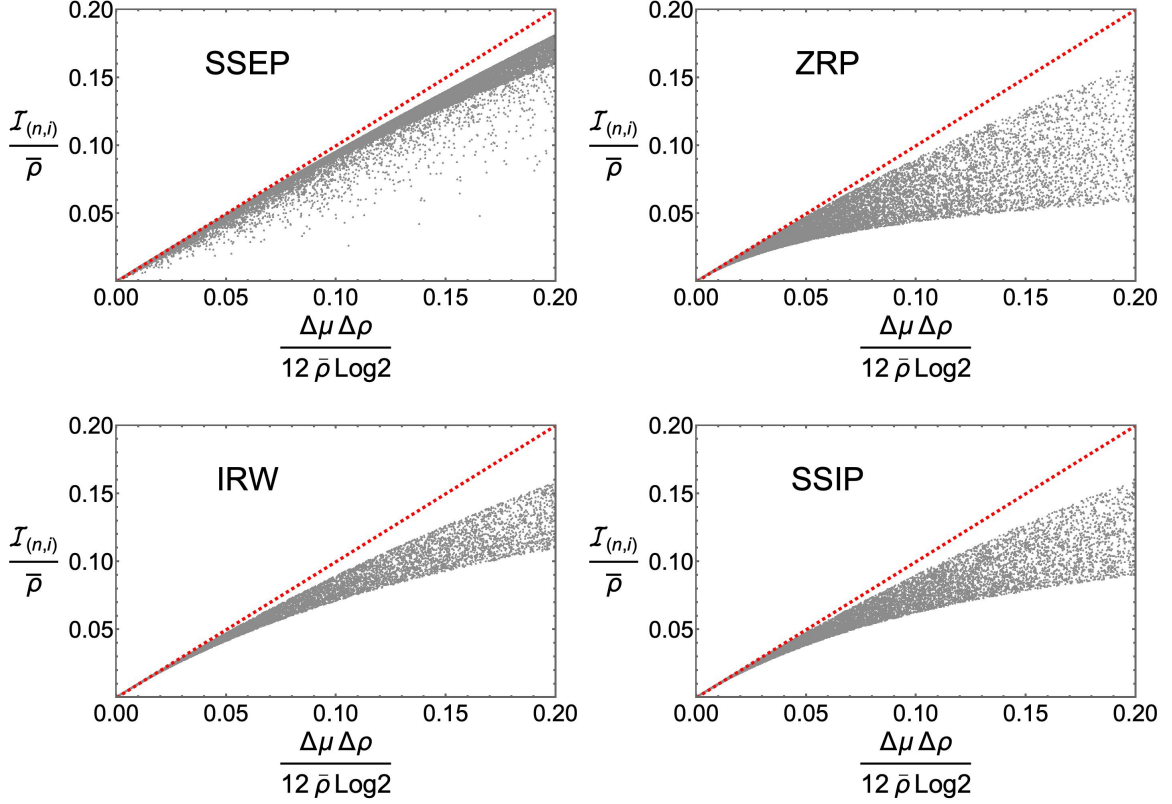


FIG. S3. In this plot, we have rescaled both sides of (S36) by  $\bar{\rho}$  and plotted  $\mathcal{I}_{(n,i)}(\bar{\rho}, \Delta\rho) / \bar{\rho}$  vs  $\Delta\mu\Delta\rho / 12\bar{\rho}\ln 2$ . As discussed below Eq. (S65), this rescaling ensures that the near-equilibrium relation (S65) is more clearly visible. The red line corresponds to the upper bound in (S36) for the flat prior case. We clearly see that the bound becomes an equality when close to equilibrium.

This matches with our general near-equilibrium expression in Eq. (S24) with  $\sigma_2(\bar{\rho}) = \bar{\rho}(1 - \bar{\rho})$ . Using this with Eq. (S59), we obtain

$$\mathcal{I}_{(n,i)}(\bar{\rho}, \Delta\rho) \approx \frac{\Delta\mu \Delta\rho}{12 \ln 2}. \quad (\text{S65})$$

This relation is valid only when  $\Delta\rho \ll \bar{\rho}$  and  $\Delta\rho \ll (1 - \bar{\rho})$ . Hence for small  $\Delta\rho$ , the upper bound (S63) becomes an equality. We have illustrated this in Figure S3 where we have plotted the two sides of (S63) along the two axes. Note that  $\Delta\mu$  will also be small when  $\bar{\rho} \gtrsim \Delta\rho$  and  $\Delta\rho \rightarrow 0^+$ . However, the relation in Eq. (S65) will no longer hold under these conditions. Therefore, for a systematic comparison, we need to normalise both sides of Eq. (S65) by  $\bar{\rho}$  and plot  $\mathcal{I}_{(n,i)}(\bar{\rho}, \Delta\rho) / \bar{\rho}$  vs  $\Delta\mu\Delta\rho / 12\bar{\rho}\ln 2$ . This rescaling ensures that Eq. (S65) will be satisfied under correct conditions.

Furthermore to make this plot, we generate a random pair of  $(\bar{\rho}, \Delta\rho)$  values by selecting  $\bar{\rho}$  uniformly from the range  $[0, 1]$ , and then choosing  $\Delta\rho$  uniformly from  $[0, \bar{\rho}]$ . Using this pair, we then calculate the positional information and  $\Delta\mu \Delta\rho$  and obtain one single data point (gray point) in top left in Figure S3. This is then repeated  $10^4$  times to get the complete plot. The red dashed line indicates our upper bound. We clearly see that the positional information remains below this red line across all parameter values.

#### IV. POSITIONAL INFORMATION FOR THE BOUNDARY DRIVEN ZRP

We now demonstrate positional information for another model, namely the open zero-range process (ZRP) and test our upper bound. The model consists of  $N$  lattice sites and each site can accommodate an arbitrary non-negative number of particles. This is different than the SSEP where each site can have at most a single particle. From any bulk site  $i$ , a particle can jump to either of its neighbouring sites with a rate  $pu_{n_i}$ , where  $u_{n_i}$  is a non-negative function of the number of particles  $n_i$ . At the boundaries ( $i = 1$  and  $i = N$ ), the dynamics are modified to allow for the addition

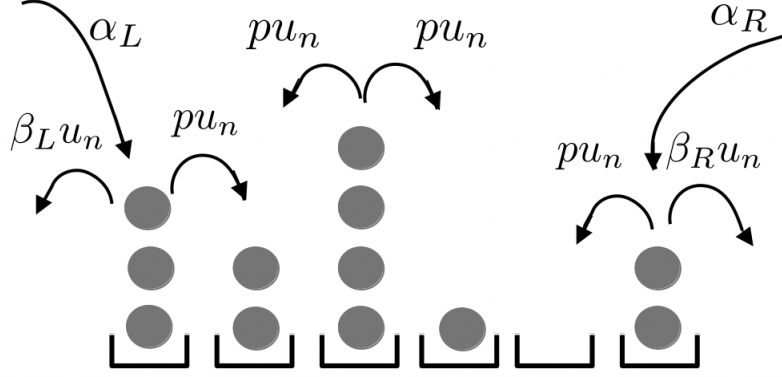


FIG. S4. Zero-range process with open boundaries

(removal) of a particle with rate  $\alpha_L$  ( $\beta_L u_{n_1}$ ) for the left boundary and with rate  $\alpha_R$  ( $\beta_R u_{n_N}$ ) for the right one (see Figure S4). Following [5], whenever steady state exists, the probability to find  $n_i = n$  number of particles in the  $i$ -th site is given by

$$P(n|i) = \mathcal{N}_i(z_i)^n \prod_{n_k=1}^n \frac{1}{u_{n_k}}, \quad \text{with } z_i = \frac{\alpha_L}{\beta_L} - \left( \frac{\alpha_L}{\beta_L} - \frac{\alpha_R}{\beta_R} \right) \left( \frac{i}{N} \right), \quad (\text{S66})$$

where  $\mathcal{N}_k$  is the normalisation factor. For the case of  $u_n = 1$ , the probability  $P(n|i)$  takes the form

$$P(n|i) = (z_i)^n (1 - z_i), \quad \text{with } z_i = \frac{\alpha_L}{\beta_L} - \left( \frac{\alpha_L}{\beta_L} - \frac{\alpha_R}{\beta_R} \right) \left( \frac{i}{N} \right). \quad (\text{S67})$$

As observed in the case of the SSEP, managing summations over  $i$  can be challenging. To simplify this, it is helpful to introduce the variable change  $x = i/N$  for large  $N$  and continue the analysis in terms of  $x$ . Rewriting Eq. (S67)

$$P(n|x) \simeq [z(x)]^n [1 - z(x)], \quad \text{with } z(x) = \frac{\alpha_L}{\beta_L} - \left( \frac{\alpha_L}{\beta_L} - \frac{\alpha_R}{\beta_R} \right) x. \quad (\text{S68})$$

Since, we are interested in calculating the positional information in terms of the variables  $\bar{\rho} = (\rho_L + \rho_R)/2$  and  $\Delta\rho = (\rho_L - \rho_R)/2$ , where  $\rho_L = \langle n(0) \rangle$  and  $\rho_R = \langle n(1) \rangle$  are average densities at the two ends

$$\rho_L = \frac{\alpha_L}{\beta_L - \alpha_L}, \quad \rho_R = \frac{\alpha_R}{\beta_R - \alpha_R}, \quad (\text{S69})$$

we rewrite Eq. (S68) in the following manner

$$P(n|x) \simeq [z(x)]^n [1 - z(x)], \quad \text{with } z(x) = c_+ - x(c_+ - c_-). \quad (\text{S70})$$

where  $c_{\pm} = (\bar{\rho} \pm \Delta\rho)/(1 + \bar{\rho} \pm \Delta\rho)$ . For this model, the average density in the bulk takes a non-linear form

$$\rho(x) = \frac{\bar{\rho}(1 + \bar{\rho}) - \Delta\rho(2x - 1 + \Delta\rho)}{(1 + \bar{\rho}) + \Delta\rho(2x - 1)}. \quad (\text{S71})$$

In the remaining part of this section, we will demonstrate that even with this non-linear profile, the bound (S36) remains still valid. To see this, we use the probability in Eq. (S70) and calculate the entropy

$$S[P(n|x)] = - \sum_{n=0}^{\infty} P(n|x) \log_2 P(n|x) = - \frac{z(x) \log_2 z(x) + (1 - z(x)) \log_2 (1 - z(x))}{(1 - z(x))}. \quad (\text{S72})$$

Taking average with respect to the prior  $P_x(x) = 1$  gives

$$\begin{aligned} & \langle S[P(n|x)] \rangle_x \\ &= - \int_0^1 dx \frac{z(x) \log_2 z(x) + (1-z(x)) \log_2 (1-z(x))}{(1-z(x))}, \\ &= - \frac{1}{\ln 2 (c_+ - c_-)} \left[ \text{Li}_2(1-c_+) - \text{Li}_2(1-c_-) - c_+ \ln c_+ + c_- \ln c_- - (1-c_+) \ln(1-c_+) + (1-c_-) \ln(1-c_-) \right], \end{aligned} \quad (\text{S73})$$

where  $\text{Li}_2(y)$  denotes the poly-logarithmic function. Next we calculate the other entropy term  $S[P_n(n)]$  in Eq. (S6) for which we need the following probability

$$P_n(n) = \int_0^1 dx P(n|x) P_x(x) = \frac{f(n)}{(c_+ - c_-)}, \quad \text{with } f(n) = \frac{c_+^{n+1} - c_-^{n+1}}{n+1} - \frac{c_+^{n+2} - c_-^{n+2}}{n+2}. \quad (\text{S74})$$

This yields

$$S[P_n(n)] = - \sum_{n=0}^{\infty} P_n(n) \log_2 P_n(n) = \log_2 (c_+ - c_-) - \frac{1}{(c_+ - c_-)} \sum_{n=0}^{\infty} f(n) \log_2 f(n). \quad (\text{S75})$$

Using Eqs. (S73) and (S75), the expression of the positional information turns out to be

$$\begin{aligned} \mathcal{I}_{(n,i)}(\bar{\rho}, \Delta\rho) &= \frac{1}{\ln 2 (c_+ - c_-)} \left[ \text{Li}_2(1-c_+) - \text{Li}_2(1-c_-) - c_+ \ln c_+ + c_- \ln c_- - (1-c_+) \ln(1-c_+) \right. \\ &\quad \left. + (1-c_-) \ln(1-c_-) - \sum_{n=0}^{\infty} f(n) \ln f(n) \right] + \log_2(c_+ - c_-). \end{aligned} \quad (\text{S76})$$

We have compared this result with the numerical simulations in Figure S1, and found a good agreement between them. Unlike in SSEP, the positional information for ZRP decreases monotonically with  $\bar{\rho}$  and vanishes for large  $\bar{\rho}$ . For larger values of  $\bar{\rho}$  but with fixed  $\Delta\rho$ , both boundary sites have a large number of particles available for hopping in the bulk, as there is no exclusion. Hence, in the steady-state, we expect the same number of particles in the bulk as well as in the boundaries. This can also be seen from Eq. (S71) where the density becomes independent of  $x$  for large enough  $\bar{\rho}$ . Therefore, the probability  $P(x|n)$  is broad with respect to  $x$ , and consequently the entropy  $S[P(x|n)]$  takes a large value. From Eq. (S4), this would mean that the positional information is small. In fact our study shows that, in processes with no exclusion,  $\mathcal{I}_{(n,i)}(\bar{\rho}, \Delta\rho)$  exhibits a monotonic decay.

Our expression in Eq. (S76) is also consistent with the one derived with perturbative approach in Eq. (S28). This can be verified by expanding Eq. (S76) in  $\Delta\rho$

$$\mathcal{I}_{(n,i)}(\bar{\rho}, \Delta\rho) \approx \frac{\Delta\rho^2}{6 \ln 2 \bar{\rho}(1+\bar{\rho})} + \frac{[3 + \bar{\rho}(11 + 7\bar{\rho})] \Delta\rho^4}{180 \ln 2 \bar{\rho}^3(1+\bar{\rho})^3}. \quad (\text{S77})$$

One essentially gets the same expression also from Eq. (S28) by plugging the central moments from Eq. (S70).

Now that we have obtained an exact expression for the positional information, we will employ it to test the bound in Eq. (S36). First, we compute the chemical potential difference using Eq. (S29) for which we need the first derivative of the free energy. In this regard, we follow a procedure similar to that of the SSEP and employ the fluctuation-response relation in Eq. (S27).

$$a_2(\bar{\rho}) = \frac{1}{\sigma_2(\bar{\rho})} = \frac{1}{\bar{\rho}(1+\bar{\rho})}, \implies a_1(\bar{\rho}) = \ln \left( \frac{\bar{\rho}}{1+\bar{\rho}} \right). \quad (\text{S78})$$

The resulting expression for  $\Delta\mu$  is now found to be

$$\Delta\mu = \ln \left( \frac{\bar{\rho} + \Delta\rho}{1 + \bar{\rho} + \Delta\rho} \right) - \ln \left( \frac{\bar{\rho} - \Delta\rho}{1 + \bar{\rho} - \Delta\rho} \right). \quad (\text{S79})$$

We now utilize these exact expressions to plot  $\mathcal{I}_{(n,i)}(\bar{\rho}, \Delta\rho)$  and  $(\Delta\mu \Delta\rho)/(12 \ln 2)$  for all possible values of  $\bar{\rho}$  and  $\Delta\rho$  in Figure S3. Here again, these quantities are rescaled by  $\bar{\rho}$  to retrieve their equality in the appropriate parameter regime. Moreover, the plot is generated in the following manner. We choose a random pair of  $(\bar{\rho}, \Delta\rho)$  values by selecting  $\bar{\rho}$  uniformly from the range  $[0, 5]$ , and then choosing  $\Delta\rho$  uniformly from  $[0, \bar{\rho}]$ . With this pair, we then calculate the positional information and  $\Delta\mu \Delta\rho$  and obtain one single data point (gray point) in top right in Figure S3. We next repeat this  $10^4$  times to get the full plot. Across all these parameter values, we see that the bound (S36) is satisfied, and it is saturated in the near-equilibrium limit. To sum up, this section showcases an example of a model with non-linear density profile, where (S36) remains valid across all parameter values.

Model	$\Delta\mu$	$\mathcal{I}_{(n,i)}(\bar{\rho}, \Delta\rho)$
SSEP	$\ln\left(\frac{\bar{\rho}+\Delta\rho}{1-\bar{\rho}-\Delta\rho}\right) - \ln\left(\frac{\bar{\rho}-\Delta\rho}{1-\bar{\rho}+\Delta\rho}\right)$	$\frac{1}{\ln 16 \Delta\rho} \left[ \mathcal{Y}(\bar{\rho}, \Delta\rho) + \mathcal{Y}(1-\bar{\rho}, \Delta\rho) - 2\Delta\rho \right] - (1-\bar{\rho}) \log_2(1-\bar{\rho}) - \bar{\rho} \log_2 \bar{\rho}$
ZRP	$\ln\left(\frac{\bar{\rho}+\Delta\rho}{1+\bar{\rho}+\Delta\rho}\right) - \ln\left(\frac{\bar{\rho}-\Delta\rho}{1+\bar{\rho}-\Delta\rho}\right)$	$\frac{1}{\ln 2(c_+ - c_-)} \left[ \text{Li}_2(1-c_+) - \text{Li}_2(1-c_-) + c_- \ln c_- - (1-c_+) \ln(1-c_+) \right. \\ \left. + (1-c_-) \ln(1-c_-) - c_+ \ln c_+ - \sum_{n=0}^{\infty} f(n) \ln f(n) \right] + \log_2(c_+ - c_-)$
IRW	$\ln(\bar{\rho} + \Delta\rho) - \ln(\bar{\rho} - \Delta\rho)$	$\frac{1}{\ln 16 \Delta\rho} \left[ \mathcal{Y}(\bar{\rho}, \Delta\rho) - 6\bar{\rho} \Delta\rho \right] - \sum_{n=0}^{\infty} \frac{g(n)}{n!} \log_2 g(n)$
SSIP	$\ln\left(\frac{\bar{\rho}+\Delta\rho}{m+\bar{\rho}+\Delta\rho}\right) - \ln\left(\frac{\bar{\rho}-\Delta\rho}{m+\bar{\rho}-\Delta\rho}\right)$	$\frac{1}{\ln 16 \Delta\rho} \left[ \mathcal{Y}(\bar{\rho}, \Delta\rho) - \mathcal{Y}(m+\bar{\rho}, \Delta\rho) + 2m \Delta\rho \right] + (m-1) \log_2 m \\ - \sum_{n=0}^{\infty} \frac{m\Gamma(m+n)}{\Gamma(n+1)\Gamma(m)} \mathcal{S}(n) \log_2 \mathcal{S}(n)$

TABLE I. Summary of the expressions of the positional information for the flat prior and chemical potential difference for different boundary-driven systems studied in the letter.

### A. Independent random walkers

In our preceding analysis, we considered a special case of zero-range process where the rate  $u_n = 1$  was chosen to be constant. We now provide another example of  $u_n = n$  where an exact expression for the positional information can be obtained and the bound can be assessed. This example corresponds to the case of independent random walkers (IRW) [5]. We use  $u_n = n$  in Eq. (S66) and obtain the conditional probability as

$$P(n|x) = \frac{[\rho(x)]^n}{n!} \exp[-\rho(x)], \quad \text{where } \rho(x) = \bar{\rho} - (2x-1)\Delta\rho, \quad (\text{S80})$$

where we have written the expression in terms of the  $x$  variable. The marginal probability  $P_n(n)$  follows to be

$$P_n(n) = \frac{g(n)}{n!}, \quad \text{with } g(n) = \frac{\Gamma(n+1, \bar{\rho} - \Delta\rho) - \Gamma(n+1, \bar{\rho} + \Delta\rho)}{2 \Delta\rho}. \quad (\text{S81})$$

We now have both probabilities required in the definition of positional information in Eq. (S6). One can now proceed in the same manner as before and calculate the two entropies as

$$S[P_n(n)] = \sum_{n=0}^{\infty} P_n(n) \log_2 n! - \sum_{n=0}^{\infty} \frac{g(n)}{n!} \log_2 g(n), \quad (\text{S82})$$

$$\langle S[P(n|x)] \rangle_x = \frac{1}{\ln 16 \Delta\rho} \left[ (\bar{\rho} - \Delta\rho)^2 \ln(\bar{\rho} - \Delta\rho) - (\bar{\rho} + \Delta\rho)^2 \ln(\bar{\rho} + \Delta\rho) + 6\bar{\rho} \Delta\rho \right] + \sum_{n=0}^{\infty} P_n(n) \log_2 n! \quad (\text{S83})$$

from which the expression of positional information can be calculated to be

$$\mathcal{I}_{(n,i)}(\bar{\rho}, \Delta\rho) = \frac{1}{\ln 16 \Delta\rho} \left[ \mathcal{Y}(\bar{\rho}, \Delta\rho) - 6\bar{\rho} \Delta\rho \right] - \sum_{n=0}^{\infty} \frac{g(n)}{n!} \log_2 g(n), \quad (\text{S84})$$

with functions  $\mathcal{Y}(\bar{\rho}, \Delta\rho)$  and  $g(n)$  defined respectively in Eqs. (S57) and (S81). Similarly, the chemical potential difference driving this system is

$$\Delta\mu = \ln(\bar{\rho} + \Delta\rho) - \ln(\bar{\rho} - \Delta\rho) \quad (\text{S85})$$

We now have at our disposal all the quantities needed to test the upper bound (S36) on the positional information. Plotting  $\mathcal{I}_{(n,i)}(\bar{\rho}, \Delta\rho) / \bar{\rho} \Delta\rho$  vs  $\Delta\mu / 12\bar{\rho} \ln 2$  in Figure S3, we have illustrated that the bound is satisfied even for this model. This model presents a third solvable example where the upper bound is valid. The data points for this model were generated using the same procedure as for the ZRP.

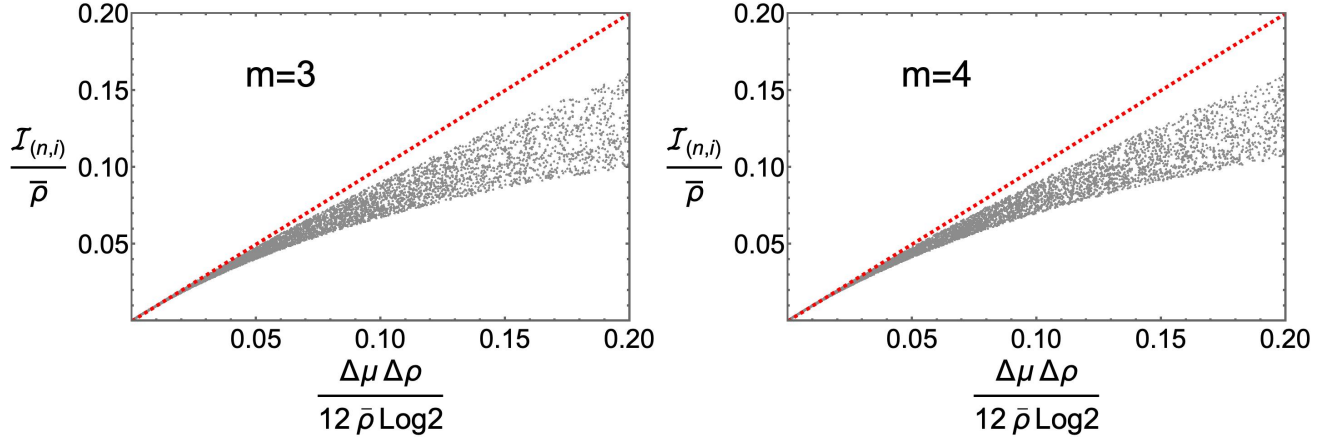


FIG. S5. Illustration of the upper bound on the positional information for SSIP model for two different values of the parameter  $m$ . The corresponding expressions of  $\mathcal{I}_{(n,i)}(\bar{\rho}, \Delta\rho)$  and  $\Delta\mu$  are given in Eqs. (S91) and (S92) respectively.

## V. POSITIONAL INFORMATION FOR THE BOUNDARY-DRIVEN SSIP

In all models examined thus far, the jump rate was either independent of the particle numbers or solely dependent on the occupation number of the source site from which the jump takes place. In this section, we will consider the SSIP model where the jump rate depends on the occupation numbers of both the source and the target sites [6, 7]. Like in ZRP, each lattice site is capable of accommodating an arbitrary non-negative number of particles. In the bulk site, a particle can jump from  $i \rightarrow j$  [with  $j = (i \pm 1)$ ] with a rate  $pn_i(n_j + m)$  where  $m (> 0)$  is a parameter in the model. At the boundaries ( $i = 1$  and  $i = N$ ), a particle can be added with rate  $\alpha_L(n_1 + m)$  for the left boundary and  $\alpha_R(n_N + m)$  for the right one. Similarly, a particle, if present, can be removed from these sites with rates  $\beta_L n_1$  and  $\beta_R n_N$  respectively. The conditional probability to observe  $n$  particles at location  $i = xN$  is [6]

$$P(n|x) = \left[ \frac{m^m \Gamma(m+n)}{n! \Gamma(m)} \right] \frac{[\rho(x)]^n}{[m + \rho(x)]^{m+n}}, \quad \text{where } \rho(x) = \bar{\rho} - (2x-1)\Delta\rho, \quad (\text{S86})$$

from which the marginal probability  $P_n(n)$  follows to be

$$P_n(n) = \frac{m \Gamma(m+n) \mathcal{S}(n)}{n! \Gamma(m)}, \quad \text{where} \quad (\text{S87})$$

$$\mathcal{S}(n) = \frac{1}{2(n+1)\Delta\rho} \left[ \left( \frac{\bar{\rho} + \Delta\rho}{m} \right)^{n+1} {}_2F_1 \left( 1+n, m+n; 2+n; -\frac{\bar{\rho} + \Delta\rho}{m} \right) - \left( \frac{\bar{\rho} - \Delta\rho}{m} \right)^{n+1} \right. \\ \left. \times {}_2F_1 \left( 1+n, m+n; 2+n; -\frac{\bar{\rho} + \Delta\rho}{m} \right) \right]. \quad (\text{S88})$$

Here  ${}_2F_1(1+n, m+n; 2+n; z)$  stands for the hypergeometric function. Now that we possess both probabilities, we can compute the two entropies to be

$$S[P_n(n)] = - \left[ \log_2 m + \sum_{n=0}^{\infty} P_n(n) \log_2 \left( \frac{\Gamma(m+n) \mathcal{S}(n)}{n! \Gamma(m)} \right) \right], \quad (\text{S89})$$

$$\langle S[P(n|x)] \rangle_x = \frac{1}{\ln 16 \Delta\rho} \left[ \mathcal{Y}(m + \bar{\rho}, \Delta\rho) - \mathcal{Y}(\bar{\rho}, \Delta\rho) - 2m \Delta\rho \right] - \sum_{n=0}^{\infty} P_n(n) \log_2 \left( \frac{\Gamma(m+n) m^m}{n! \Gamma(m)} \right). \quad (\text{S90})$$

Using these two expressions, the positional information can be calculated to be

$$\mathcal{I}_{(n,i)}(\bar{\rho}, \Delta\rho) = \frac{1}{\ln 16 \Delta\rho} \left[ \mathcal{Y}(\bar{\rho}, \Delta\rho) - \mathcal{Y}(m + \bar{\rho}, \Delta\rho) + 2m \Delta\rho \right] + (m-1) \log_2 m - \sum_{n=0}^{\infty} \frac{m \Gamma(m+n) \mathcal{S}(n)}{\Gamma(n+1)\Gamma(m)} \log_2 \mathcal{S}(n), \quad (\text{S91})$$

with functions  $\mathcal{Y}(\bar{\rho}, \Delta\rho)$  and  $\mathcal{S}(n)$  given respectively in Eq. (S57) and (S88). Similarly, the chemical potential difference driving the system is

$$\Delta\mu = \ln\left(\frac{\bar{\rho} + \Delta\rho}{m + \bar{\rho} + \Delta\rho}\right) - \ln\left(\frac{\bar{\rho} - \Delta\rho}{m + \bar{\rho} - \Delta\rho}\right). \quad (\text{S92})$$

We are now equipped with all the necessary elements to assess the upper bound (S36) on positional information. In Figure S3, we have again plotted  $\mathcal{I}_{(n,i)}(\bar{\rho}, \Delta\rho) / \bar{\rho}\Delta\rho$  vs  $\Delta\mu / 12\bar{\rho}\ln 2$  for  $m = 2$  for different values of  $\Delta\rho$  and  $\bar{\rho}$ . The data points for this model were generated using the same procedure as for the ZRP. Across all these values, we once again find that our bound is satisfied. We have also verified this for other values of  $m$  in Figure S5. This consistency further reinforces the conjecture that our bound holds for general boundary-driven systems.

## VI. NON-FLAT PRIOR

In all the toy models studied above, we consider the case of a flat prior and numerically demonstrated the upper bound (S36). On the other hand, for a general prior, we proved that the near-equilibrium positional information satisfies a universal upper bound (S35). In this section, we will test the validity of this bound for the toy examples when the system is significantly far from the equilibrium.

Following the same steps as presented before, one can obtain the positional information for a general prior  $P_x(x)$  to be

$$\begin{aligned} \mathcal{I}_{(n,i)}(\bar{\rho}, \Delta\rho) \Big|_{\text{SSEP}} &= \int_0^1 dx P_x(x) [\rho(x) \log_2 \rho(x) + (1 - \rho(x)) \log_2 (1 - \rho(x))] - \rho_{\text{ss}} \log_2 \rho_{\text{ss}} - (1 - \rho_{\text{ss}}) \log_2 (1 - \rho_{\text{ss}}), \\ \mathcal{I}_{(n,i)}(\bar{\rho}, \Delta\rho) \Big|_{\text{ZRP}} &= \int_0^1 dx P_x(x) \left[ \frac{z(x) \log_2 z(x) + (1 - z(x)) \log_2 (1 - z(x))}{z(x)} \right] - \sum_{n=0}^{\infty} \mathcal{G}_{\text{ZRP}}(n) \log_2 \mathcal{G}_{\text{ZRP}}(n), \\ \mathcal{I}_{(n,i)}(\bar{\rho}, \Delta\rho) \Big|_{\text{IRW}} &= \frac{1}{\ln 2} \int_0^1 dx P_x(x) \rho(x) (\ln \rho(x) - 1) - \sum_{n=0}^{\infty} \frac{\mathcal{G}_{\text{IRW}}(n)}{n!} \log_2 \mathcal{G}_{\text{IRW}}(n), \\ \mathcal{I}_{(n,i)}(\bar{\rho}, \Delta\rho) \Big|_{\text{SSIP}} &= \int_0^1 dx P_x(x) [\rho(x) \log_2 \rho(x) - (m + \rho(x)) \log_2 (m + \rho(x))] - \sum_{n=0}^{\infty} \frac{\Gamma(m+n) \mathcal{G}_{\text{SSIP}}(n)}{m^{-m} n! \Gamma(m)} \log_2 \mathcal{G}_{\text{SSIP}}(n), \end{aligned} \quad (\text{S93})$$

where the different functions appearing in these expressions are defined as follows

$$\begin{aligned} \rho(x) &= \bar{\rho} + (1 - 2x)\Delta\rho, \quad \rho_{\text{ss}} = \int_0^1 dx P_x(x) \rho(x), \quad z(x) = \frac{\bar{\rho} + \Delta\rho}{1 + \bar{\rho} + \Delta\rho} - x \left( \frac{\bar{\rho} + \Delta\rho}{1 + \bar{\rho} + \Delta\rho} - \frac{\bar{\rho} - \Delta\rho}{1 + \bar{\rho} - \Delta\rho} \right), \\ \mathcal{G}_{\text{ZRP}}(n) &= \int_0^1 dx P_x(x) z(x)^n (1 - z(x)), \quad \mathcal{G}_{\text{IRW}}(n) = \int_0^1 dx P_x(x) \rho(x)^n e^{-\rho(x)}, \quad \mathcal{G}_{\text{SSIP}}(n) = \int_0^1 dx \frac{P_x(x) \rho(x)^n}{(m + \rho(x))^{m+n}}. \end{aligned}$$

Note that the exact expressions are for  $v_c = 1$  and  $k_B T = 1$ . Furthermore, the chemical potential difference  $\Delta\mu$  for these models are given in Table I. Using these results, we have tested the inequality (S35) in Figure S6 for different choices of  $P_x(x)$ . The prior  $P_x(x)$  is sampled as

$$P_x(x) = \frac{\sum_{\ell=0}^s \kappa_{\ell} x^{\mu_{\ell}}}{\sum_{\ell=0}^s \frac{\kappa_{\ell}}{\mu_{\ell} + 1}}, \quad (\text{S94})$$

with  $s = 10$ . We generate random values of  $\kappa_{\ell}$  and  $\mu_{\ell}$  by drawing  $\kappa_{\ell}$  from a uniform distribution  $[0, 5]$  and  $\mu_{\ell}$  from another uniform distribution  $[-1, 6]$ , independently for each value of  $\ell$ . This gives us a random  $P_x(x)$ . Other parameters  $\bar{\rho}$  and  $\Delta\rho$  are obtained using the same procedure as before. Using these, we obtain one data point (gray symbol) in Figure S6. This procedure is then repeated  $5 \times 10^3$  times for each model. For better visibility of the plot, we have again rescaled both sides of (S35) by  $\bar{\rho}$  and plotted  $\mathcal{I}_{(n,i)}(\bar{\rho}, \Delta\rho) / \bar{\rho}$  vs  $\Delta\mu\Delta\rho / 4\bar{\rho}\ln 2$ . Figure S6 clearly demonstrates that (S35) is satisfied even in the non-equilibrium regime.

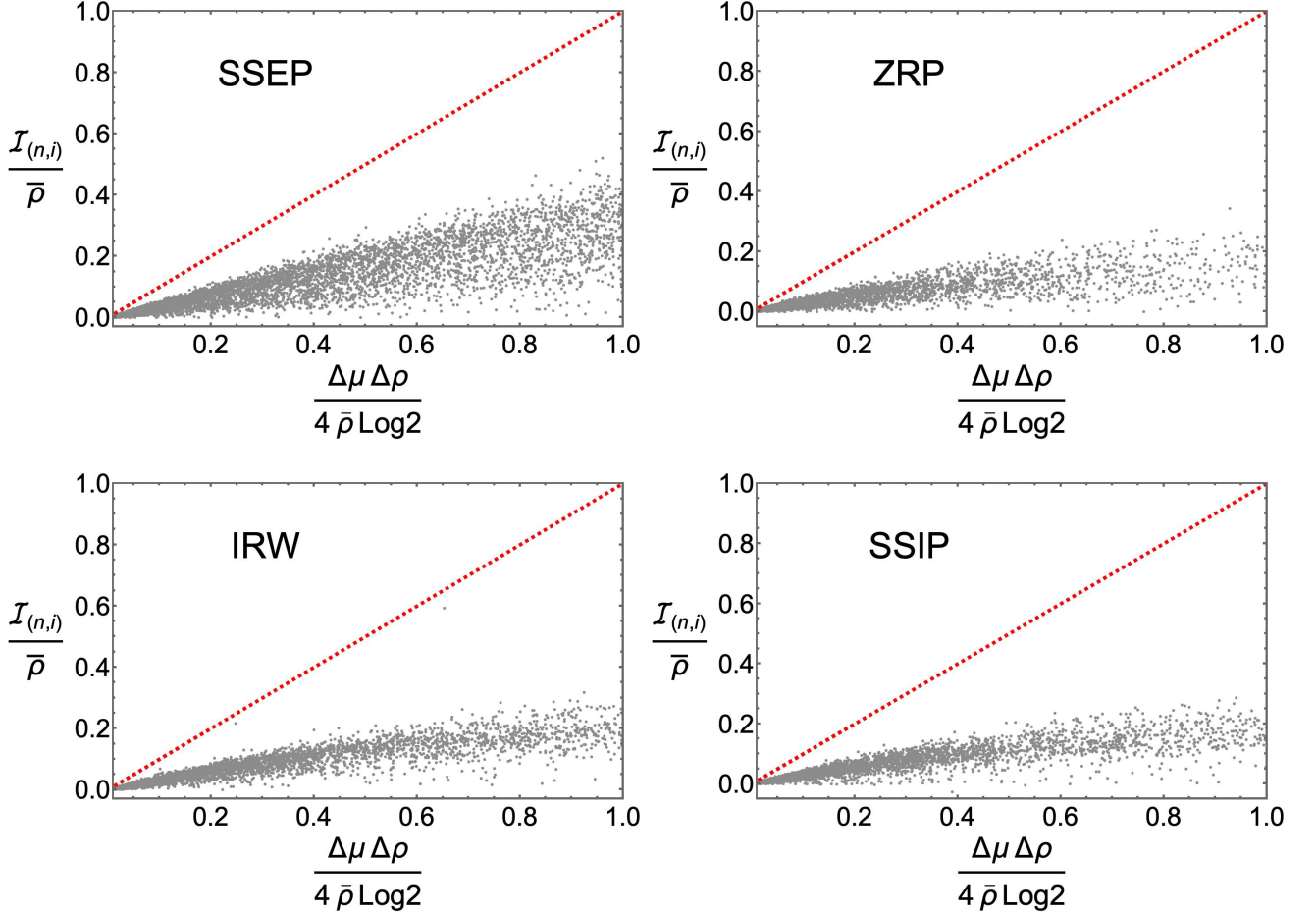


FIG. S6. We have plotted  $\mathcal{I}_{(n,i)}(\bar{\rho}, \Delta\rho) / \bar{\rho}$  vs  $\Delta\mu\Delta\rho / 4\bar{\rho}\ln 2$  for all four models to test the inequality (S35). For each data point, the prior probability is randomly generated by following the procedure in Eq. (S94). We clearly see that (S35) is satisfied even in the strongly non-equilibrium regime.

## VII. HIGHER DIMENSION

In this section, we show that the perturbative method developed in section II can also be extended to higher dimensional models. We consider a  $d$ -dimensional lattice system graph whose sites are labelled by the index  $\vec{i} = (i_1, i_2, \dots, i_d)$ . As shown in Figure S7, the system is connected to two reservoirs  $\rho_L$  and  $\rho_R$  respectively at  $\vec{i}_L = (1, i_2, i_3, \dots, i_d)$  and  $\vec{i}_R = (N, i_2, i_3, \dots, i_d)$  with  $N$  being the separation between the two reservoirs. Such a scenario also arises in experiments where an embryo has morphogen inputs and outputs at its two poles [1]. At other sites, a particle can jump symmetrically to any of its neighbouring sites following some dynamical rule.

When  $\rho_L$  and  $\rho_R$  are well separated, i.e.  $N$  is large, we anticipate the local equilibrium to hold true even in this higher dimensional set-up. Then the probability density to observe a density  $g$  in a small volume  $v_c$  at site  $\vec{i}$  is

$$P(g|\vec{i}) \sim \exp \left[ -\frac{v_c}{k_B T} \left( \mathcal{G}_{\mu_{\vec{i}}} (g) - \mathcal{G}_{\mu_{\vec{i}}} (\rho_{\vec{i}}) \right) \right], \quad (\text{S95})$$

where  $\rho_{\vec{i}}$  and  $\mu_{\vec{i}}$  are the local average density and local chemical potential and  $\mathcal{G}_{\mu_{\vec{i}}}(g)$  is given in terms of the Helmholtz free energy  $a(g)$  per unit volume as

$$\mathcal{G}_{\mu_{\vec{i}}}(g) = a(g) - \mu_{\vec{i}} g \quad \text{and} \quad \mu_{\vec{i}} = \left. \frac{\partial a(g)}{\partial g} \right|_{g=\rho_{\vec{i}}}. \quad (\text{S96})$$

As discussed in the one-dimensional case, the precise form of  $\rho_{\vec{i}}$  depends on the specific model. Yet it is possible to perform an expansion of  $\rho_{\vec{i}}$  to capture the leading near-equilibrium behaviour. The first two terms in this expansion

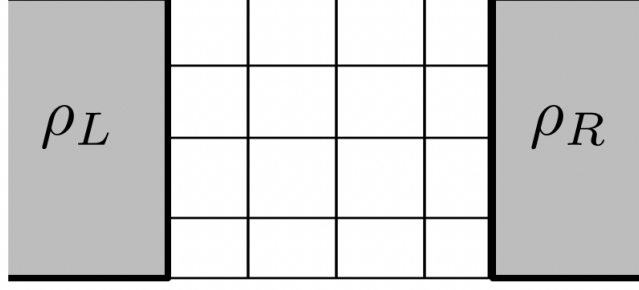


FIG. S7. Higher dimensional lattice system with two particle reservoirs at densities  $\rho_L$  and  $\rho_R$ . At other sites, a particle can jump symmetrically to any of its neighbouring sites with some rate.

are

$$\rho_{\vec{i}} \approx \bar{\rho} + \left(1 - \frac{2i_1}{N}\right) \Delta\rho + \mathcal{L}_2(\vec{i}, \bar{\rho}) \Delta\rho^2. \quad (\text{S97})$$

To write the coefficient of the linear  $\Delta\rho$  term, we use the symmetry that the density should remain invariant under the transformation  $\rho_L \leftrightarrow \rho_R$  and  $(i_1, i_2, i_3, \dots, i_d) \rightarrow (N - i_1, i_2, i_3, \dots, i_d)$ . Moreover it should be independent of  $i_2, i_3, \dots, i_d$  according to the diffusion equation.

Plugging this form of density in Eq. (S95), we can proceed exactly as in section II and obtain

$$\mathcal{I}_{(n, \vec{i})}(\bar{\rho}, \Delta\rho) \leq \frac{\Delta\mu v_c \Delta\rho}{4 k_B T \ln 2}. \quad (\text{S98})$$

This is a universal bound valid for any choice of prior as long as the system is near equilibrium.

### VIII. PROOF OF THE RELATIONS IN EQ. (S27)

For a system in equilibrium, we stated some relations in Eq. (S27) that give central moments of the density in terms of the derivatives of the associated free energy. Here, we present a mathematical proof of these relations. Note that the probability distribution to observe a density  $n$  inside a volume  $v_c$  at equilibrium is given by

$$P_{\text{eq}}(n) = \frac{e^{-\frac{v_c}{k_B T} [a(n) - a(\bar{\rho}) - \bar{\mu}(n - \bar{\rho})]}}{\int dn e^{-\frac{v_c}{k_B T} [a(n) - a(\bar{\rho}) - \bar{\mu}(n - \bar{\rho})]}}, \quad (\text{S99})$$

where  $\bar{\rho} = \langle n \rangle_{\text{eq}}$  is the average density, and  $\bar{\mu}$  is the chemical potential related to  $\bar{\rho}$  by

$$\bar{\mu} = \frac{da(\bar{\rho})}{d\bar{\rho}}. \quad (\text{S100})$$

For simplicity, we choose  $k_B T = 1$  and  $v_c = 1$ . Eq. (S99) can be further simplified as

$$P_{\text{eq}}(n) = \frac{\exp[-a(n) + \bar{\mu}n]}{Z_P}, \quad \text{with } Z_P = \int dn \exp[-a(n) + \bar{\mu}n]. \quad (\text{S101})$$

Any moment of the density can be computed by taking the derivative of the partition function  $Z_P$

$$\langle n^k \rangle_{\text{eq}} = \frac{1}{Z_P} \frac{\partial^k Z_P}{\partial \bar{\mu}^k}. \quad (\text{S102})$$

### A. Variance of $n$

Putting  $k = 2$  in Eq. (S102), we get the second moment

$$\langle n^2 \rangle_{\text{eq}} = \frac{1}{Z_P} \frac{\partial^2 Z_P}{\partial \bar{\mu}^2} = \frac{\partial}{\partial \bar{\mu}} \left[ \frac{1}{Z_P} \frac{\partial Z_P}{\partial \bar{\mu}} \right] + \left[ \frac{1}{Z_P} \frac{\partial Z_P}{\partial \bar{\mu}} \right]^2. \quad (\text{S103})$$

Now identifying  $\left[ \frac{1}{Z_P} \frac{\partial Z_P}{\partial \mu_L} \right] = \bar{\rho}$ , one can rewrite the above expression as

$$\sigma_2(\bar{\rho}) \equiv \langle n^2 \rangle_{\text{eq}} - \bar{\rho}^2 = \frac{d\bar{\rho}}{d\bar{\mu}}. \quad (\text{S104})$$

To simplify further, we take  $\bar{\mu}$  from Eq. (S100) and take its derivative with  $\bar{\rho}$  to get  $a_2(\bar{\rho}) = \frac{d\bar{\mu}}{d\bar{\rho}}$ . Plugging this in Eq. (S104) yields

$$\sigma_2(\bar{\rho}) = \frac{1}{a_2(\bar{\rho})}. \quad (\text{S105})$$

This relation gives us the equilibrium variance of the density in terms of the underlying free energy of the system.

### B. Third central moment of $n$

We next look at the third moment for which we put  $k = 3$  in Eq. (S102). This gives

$$\begin{aligned} \langle n^3 \rangle_{\text{eq}} &= \frac{1}{Z_P} \frac{\partial^3 Z_P}{\partial \bar{\mu}^3} = \frac{1}{Z_P} \frac{\partial}{\partial \bar{\mu}} \left[ Z_P \langle n^2 \rangle_{\text{eq}} \right], \\ &= \bar{\rho} \langle n^2 \rangle_{\text{eq}} + \frac{\partial \langle n^2 \rangle_{\text{eq}}}{\partial \bar{\mu}}. \end{aligned} \quad (\text{S106})$$

To evaluate the derivative with  $\bar{\mu}$ , we use Eqs. (S100) and (S104) as  $\frac{\partial \langle n^2 \rangle_{\text{eq}}}{\partial \bar{\mu}} = \frac{\partial \langle n^2 \rangle_{\text{eq}}}{\partial \bar{\rho}} \frac{d\bar{\rho}}{d\bar{\mu}} = \sigma_2(\bar{\rho}) \frac{\partial \langle n^2 \rangle_{\text{eq}}}{\partial \bar{\rho}}$ . Furthermore, we also write  $\langle n^2 \rangle_{\text{eq}} = \sigma_2(\bar{\rho}) + \bar{\rho}^2$ . The expression of  $\langle n^3 \rangle_{\text{eq}}$  then becomes

$$\langle n^3 \rangle_{\text{eq}} = 3\bar{\rho} \sigma_2(\bar{\rho}) + \bar{\rho}^3 + \sigma_2(\bar{\rho}) \frac{\partial \sigma_2(\bar{\rho})}{\partial \bar{\rho}}. \quad (\text{S107})$$

With this expression, the third central moment  $\sigma_3(\bar{\rho}) = \langle (n - \bar{\rho})^3 \rangle_{\text{eq}}$  turns out to be

$$\sigma_3(\bar{\rho}) = \sigma_2(\bar{\rho}) \frac{\partial \sigma_2(\bar{\rho})}{\partial \bar{\rho}} = -\sigma_2(\bar{\rho})^3 a_3(\bar{\rho}), \quad (\text{S108})$$

where for the second equality, we have used Eq. (S105). Proceeding in the same, one can show that the fourth central moment is

$$\sigma_4(\bar{\rho}) = -\sigma_2(\bar{\rho})^4 a_4(\bar{\rho}) + \frac{3}{\sigma_2(\bar{\rho})} \left[ \sigma_3(\bar{\rho})^2 + \sigma_2(\bar{\rho})^3 \right]. \quad (\text{S109})$$

## IX. DERIVATION OF THE HELMHOLTZ FREE ENERGY

Here, will derive the expression for the Helmholtz free energy  $a(g)$  per unit volume. For simplicity, we will focus on the zero-range process, as the mathematical procedure for other models is essentially the same. From Eq. (S27), we see that the second derivative of  $a(\bar{\rho})$  is related to the variance of density  $\sigma_2(\bar{\rho}) = \langle g^2 \rangle - \bar{\rho}^2$  in equilibrium. Thus, we begin with the computation of the variance.

At equilibrium, the entire system has the same density including at the boundaries  $\rho_L = \rho_R = \bar{\rho}$ , and the probability to observe a density  $g = n/v_c$  about a small volume  $v_c$  of a lattice site follows from Eq. (S70) to be

$$P(g) = \frac{(v_c \bar{\rho})^{g v_c}}{(1 + v_c \bar{\rho})^{g v_c + 1}}, \quad \text{with } g = 0, \frac{1}{v_c}, \frac{2}{v_c}, \frac{3}{v_c}, \dots \quad (\text{S110})$$

Here  $\bar{\rho} = \langle g \rangle$  and is related to the model parameters as

$$v_c \bar{\rho} = \frac{\alpha_L}{\beta_L - \alpha_L} = \frac{\alpha_R}{\beta_R - \alpha_R}, \quad (\text{S111})$$

The density variance is

$$\sigma_2(\bar{\rho}) = \bar{\rho} \left( \frac{1}{v_c} + \bar{\rho} \right). \quad (\text{S112})$$

Using Eq. (S27)

$$\frac{a_2(\bar{\rho})}{k_B T} = \frac{1}{\bar{\rho}(1 + v_c \bar{\rho})}. \quad (\text{S113})$$

The integration with respect to  $\bar{\rho}$  gives

$$\frac{a_1(\bar{\rho})}{k_B T} = \ln(v_c \bar{\rho}) - \ln(1 + v_c \bar{\rho}) + \mathbb{M}, \quad (\text{S114})$$

where  $\mathbb{M}$  is the integration constant. To evaluate it, we first note that when  $\bar{\rho} \rightarrow \infty$ , Eq. (S111) gives  $\alpha_L \rightarrow \beta_L$ . This means that  $\bar{\rho} \rightarrow 0$  is possible when the chemical potential  $\mu_L \sim \ln(\alpha_L/\beta_L)$  goes to zero. Since  $a_1(\bar{\rho})$  is related to the chemical potential through Eq. (S10), we must have  $a_1(\bar{\rho} \rightarrow \infty) = 0$ . Plugging this in Eq. (S114) then gives  $\mathbb{M} = 0$ .

Performing one more integration

$$\frac{a(\bar{\rho})}{k_B T} = \bar{\rho} \ln(v_c \bar{\rho}) - \left( \frac{1}{v_c} + \bar{\rho} \right) \ln(1 + v_c \bar{\rho}). \quad (\text{S115})$$

This gives us the Helmholtz free energy  $a(\bar{\rho})$  per unit volume for the ZRP model. The same analysis can be repeated for other models as well and the results can be summarised as follows

$$\frac{a(\bar{\rho})}{k_B T} = \begin{cases} \bar{\rho} \ln(v_c \bar{\rho}) + (1/v_c - \bar{\rho}) \ln(1 - v_c \bar{\rho}), & \text{SSEP} \\ \bar{\rho} \ln(v_c \bar{\rho}) - \left( \frac{1}{v_c} + \bar{\rho} \right) \ln(1 + v_c \bar{\rho}), & \text{ZRP} \\ \bar{\rho} \ln(v_c \bar{\rho}) - \bar{\rho}, & \text{IRW} \\ \bar{\rho} \ln(v_c \bar{\rho}) - \left( \frac{m}{v_c} + \bar{\rho} \right) \ln(m + v_c \bar{\rho}). & \text{SSIP} \end{cases}$$

- 
- [1] J. O. Dubuis, G. Tkačik, E. F. Wieschaus, T. Gregor, and W. Bialek, Positional information, in bits, [Proceedings of the National Academy of Sciences](#) **110**, 16301 (2013).
  - [2] L. Wolpert, Positional information and the spatial pattern of cellular differentiation, [Journal of Theoretical Biology](#) **25**, 1 (1969).
  - [3] B. Derrida, J. L. Lebowitz, and E. R. Speer, Free energy functional for nonequilibrium systems: An exactly solvable case, [Physical Review Letters](#) **87**, 150601 (2001).
  - [4] B. Derrida, J. L. Lebowitz, and E. R. Speer, Large deviation of the density profile in the steady state of the open symmetric simple exclusion process, [Journal of Statistical Physics](#) **107**, 599 (2002).
  - [5] E. Levine, D. Mukamel, and G. M. Schütz, Zero-range process with open boundaries, [Journal of Statistical Physics](#) **120**, 759 (2005).
  - [6] K. Vafayi and M. H. Duong, Weakly nonequilibrium properties of a symmetric inclusion process with open boundaries, [Physical Review E](#) **90**, 052143 (2014).
  - [7] C. Franceschini, P. Gonçalves, and F. Sau, Symmetric inclusion process with slow boundary: Hydrodynamics and hydrostatics, [Bernoulli](#) **28**, 1340 (2022).